U.S. Department of Energy
Office of Advanced Automotive Technologies
1000 Independence Avenue S.W.
Washington, D.C. 20585-01211

FY 2000

Oak Ridge National Laboratory
Progress Report for the Power Electronics and Electric Machinery Program

D. J. Adams
ORNL Program Manager

Submitted to:

Energy Efficiency Renewable Energy
Office of Transportation Technologies
Office of Advanced Automotive Technologies
Energy Management Team

Raymond Sutula Energy Management Team Leader

CONTENTS

ACRONYMS

AC	Alternating Current
AIPM	Automotive Integrated Power Module
ART	Auxiliary Resonant Tank
BDCM	Brushless DC Machine
CPSR	Constant Power Speed Ratio
dc	Direct Current
DLL	Dynamic Link Library
DMIC	Dual Mode Inverter Control
DOE	Department of Energy
DSP	Digital Signal Processor
EE/TT	Electrical and Electronics Technical Team
EMI	Electromagnetic Interference
FUDS	Federal Urban Driving Schedule
FHDS	Federal Highway Driving Schedule
HEV	Hybrid Electric Vehicle
ICE	Internal Combustion Engine
IGBT	Insulated Gate Bipolar Transistor
MOSFET	Metal Oxide Semiconductor type Field-Effect Transistor
MEMS	Microelectromechanical Systems
NTRC	National Transportation Research Center
OAAT	Office of Advanced Automotive Technology
OEM	Original Equipment Manufacturer
ORNL	Oak Ridge National Laboratory
PM	Permanent Magnet
PMSM	PM Synchronous Machines
PNGV	Partnership for a New Generation of Vehicles
PWM	Pulse Width Modulation
R&D	Research and Development
RGPM	Radial Gap Permanent Magnet
RMS	Root Mean Square
RSI	Resonant Snubber Inverter
RTW	Real-Time Workshop
SCR	Silicon Controlled Rectifier
SRM	Switched Reluctance Motor
SSS	Soft-Switching Snubbered
THD	Total Harmonic Distortion
TTL	Transistor-Transistor Logic

A. Inverter/Converter Topologies and Packaging Research and Development (R&D)

Fang Z. Peng
Oak Ridge National Laboratory
National Transportation Research Center
2360 Cherahala Boulevard
Knoxville, Tennessee 37932
Voice: 865-946-1323; Fax: 865-946-1210; pengfz@ornl.gov

Objectives

- Develop advanced inverter/converter topologies and new packaging techniques for automotive applications to increase efficiency, reduce costs, and increase reliability to meet the Partnership for a New Generation of Vehicles (PNGV) goals.
- Focus on the development of multilevel inverter topologies/controls, soft-switching inverter (SSI) topologies, direct current (dc)/dc converters, and their packaging.

Approach

- Develop and demonstrate the new soft switching topology using only passive components.
- Prototype the new isolated bi-directional dc/dc converter for fuel cell vehicles.
- Develop self-powered gate drive circuit for multilevel inverters and integrate it into the inverter module, and demonstrate cost reduction and high reliability for low voltage traction drives.
- Investigate a novel multilevel dc/dc converter for dual-voltage systems.

Accomplishments

- A new soft switching technology, soft-switching snubbered (SSS) inverter, using only passive components to achieve soft switching without the increase of cost and control complication, has been developed and fabricated. Simulation studies showed the feasibility and operation. A 100 kW prototype has been built.
- A 5kW dc-dc converter prototype has been built. Initial results demonstrated the following features: (1) minimum number (only four) of switching devices compared with (eight or nine) the traditional bi-directional isolated power converters; (2) over 30% costs reduction; and (3) over 40% volume reduction.
- A 2kW multilevel inverter cell has been built and tested successfully. A newly developed self-powered gate drive circuit was integrated into the inverter cell, which only requires transistor-transistor logic (TTL) gate signals and dc link connections. The prototype and test results demonstrated the feasibility, compactness, and cost reduction.

Future Directions

- Test and demonstrate the 100 kW SSS inverter prototype.

- Test the 5 kW soft-switching dc-dc converter and measure efficiency at different operating points.
- Fabricate a multilevel inverter using the developed 2 kW multilevel inverter cells and demonstrate its feasibility for hybrid electric vehicle (HEV) drives. Complete a 30 kW prototype and test with a motor to confirm the high efficiency, no electromagnetic interference (EMI), and high reliability features.
- Prototype a bi-directional dc-dc converter using the developed 2 kW multilevel inverter cells for 42/14V dual voltage systems.

Introduction

The Oak Ridge National Laboratory (ORNL) has developed a series of advanced soft-switching inverter topologies based on auxiliary resonant techniques. These topologies include the resonant snubber inverter (RSI) and auxiliary resonant tank (ART) inverter. ORNL has successfully applied the RSI technology into a super-conducting coil control system for medical applications. ART inverter prototypes (10kW and 100kW) have successfully demonstrated the superiority and has been applied to an electric bus drive application.

However, all existing SSIs (including ORNL's) use additional active devices to achieve soft-switching, thus increasing costs and complexity and decreasing reliability. This project investigates regenerative snubber circuits and develops a new soft switching technology (SSS inverter). The SSS inverter uses only passive components to achieve soft-switching without the increase of cost and control complication.

Bi-directional dc/dc converters with isolation have been a demanded development for many applications including fuel cell vehicles, etc. The traditional dc/dc converters with isolation and bi-directional power flow have the following disadvantages: (1) two separate full converter bridges are needed, resulting in an excessive component count and high costs; (2) transformer leakage causes surge voltage, power losses, and control difficulties; (3) a clamping circuit or snubber circuit is required; and (4) hard-switching related problems, such as high EMI, high dV/dt, etc., require sophisticated filters and shielding. A new dc/dc converter has been proposed at ORNL. The new converter uses a minimum number (only four) of switching devices compared with (eight or nine) the traditional bi-directional isolated power converters, thus reducing costs tremendously. The new converter provides soft switching as a by-product of the topology without any penalty. It is very suited for dc/dc and dc/dc/alternating current (ac) power conversion where isolation, voltage boost, and bi-directional power flow are required. Therefore, the new converter especially has a niche in HEV/fuel cell applications, energy storage systems, etc. Simulations and design for a 5 kW prototype have been finished and this year's focus is on prototyping and demonstration.

ORNL has done a lot of pioneer work on multilevel inverters. The project explores these topologies and develops new control strategies and new gate drive circuits. A 10kW 21-level inverter has been built to demonstrate the feasibility of the topology and control. Through the newly developed gate drive circuit, a 30 kW prototype is being fabricated to demonstrate cost reduction and the feasibility of low voltage (<50V) traction drives. In addition, this project investigates a new multilevel dc/dc converter without any magnetics for dual-voltage systems.

SSS Inverter

The proposed SSS inverter is aiming at the following goals:

1. Minimize additional cost for achieving soft switching;
2. Operate like a hard-switching inverter, with no limitations and no control complications; and
3. Reliable and efficient.

To achieve those goals, the SSS inverter: (1) only uses passive components, (2) requires no additional control, (3) can employ any PWM control without difficulties, (4) needs no dc bus plane, (5) utilizes parasitics, (6) reduces dv/dt and di/dt passively, and (7) only needs low-cost and more reliable components. Figure A-1 shows a single phase leg insulated gate bipolar transistor (IGBT) module and a SSS module. The SSS module is supposed to be mounted right on the top of the IGBT module. Simulation study showed the feasibility and operation. Figure A-2 shows waveforms that confirms soft turn-on and soft turn-off operations. The voltage change rate dV/dt and switching losses are well suppressed and reduced. A 100 kW prototype has been built and tests are underway.

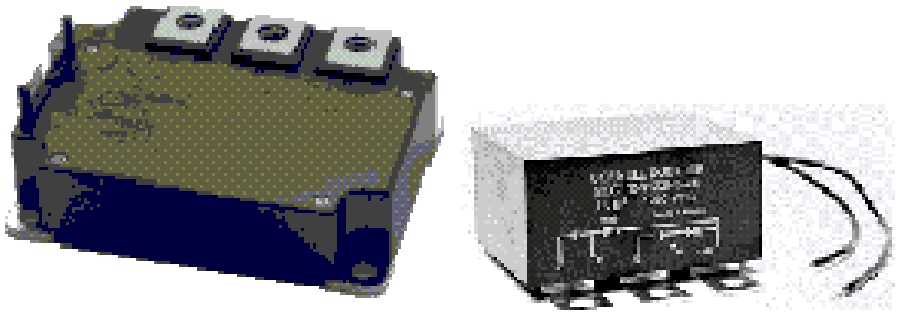

Figure A-1. IGBT and SSS modules.

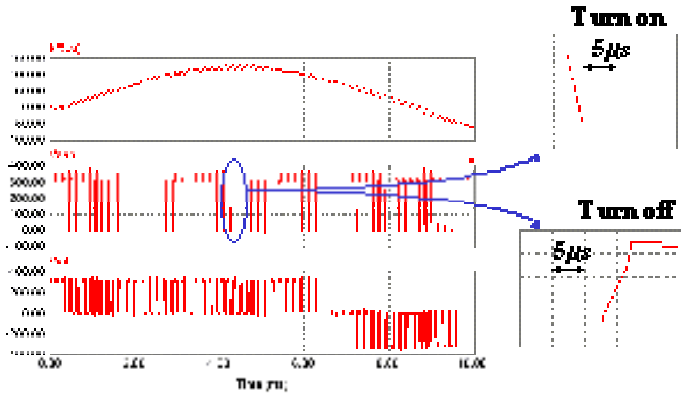

Figure A-2. Simulation waveforms of SSS inverter.

Bi-directional DC-DC Converter

There are very few topologies and products available for bi-directional dc-dc converters. Bi-directional dc-dc converters are usually high cost and have an excessive number of components. For fuel cell vehicle applications, the challenges faced in the development of dc-dc converters are (1) a high power and high current, (2) high voltage ratio, (3) bi-directional power flow, and (4) low cost and high reliability. This task is focussing on the development of a new bi-directional dc-dc converter. Figure A-3 shows the new converter's topology. Compared with the state-of-the-art dc-dc converter developed before, the new dc-dc converter has the following advantages: half component count, soft-switching without additional cost, more compact, light weight, and reliable, low cost, and less control/accessories. Figure A-4 is a photo of the prototyped 5kW dc-dc converter. Obviously, over 40% volume and 30% cost reductions have been achieved. Full load testing is underway.

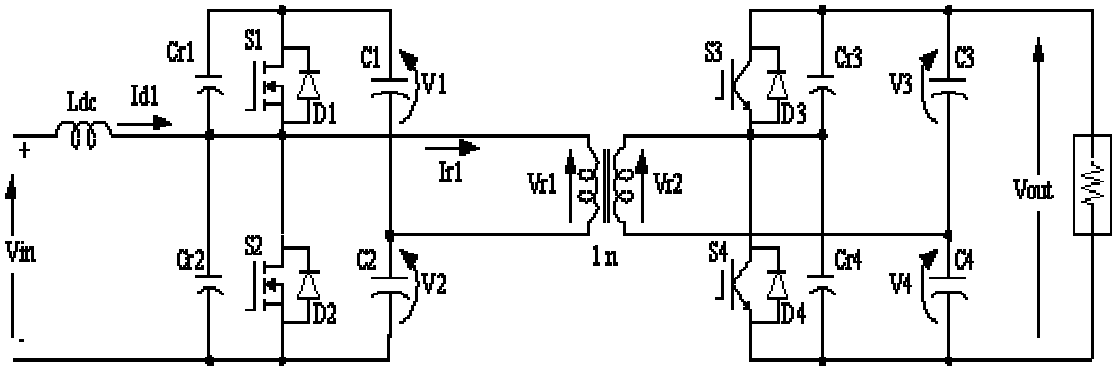

Figure A-3. New dc-dc converter topology.

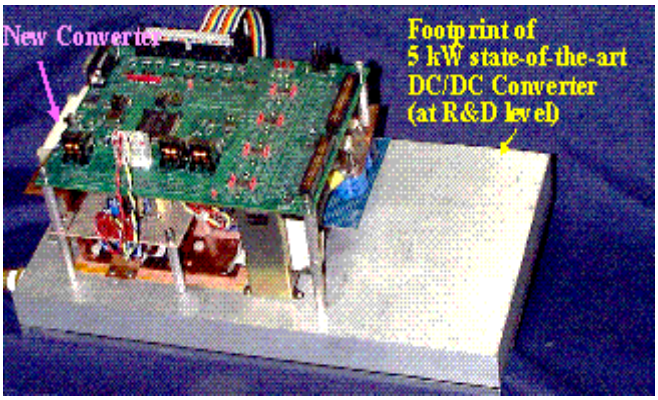

Figure A-4. DC-dc converter prototype.

Multilevel Inverter Cell

ORNL has proposed multilevel inverters for motor drive and utility applications. The main features of multilevel inverters are: extremely high efficiency (≥ 99% over 10-100% load); extremely low total harmonic distortion (THD) in both the voltage and current; almost no EMI,

3-order (60dB) less than 10kHz PWM inverters; low dc voltage (<50V), open wiring possible and no safety hazard; and low cost and high reliability if a smart gate drive circuit and integration/packaging technique is developed.

A new self-powered gate drive circuit has been developed and integrated into a multilevel inverter cell, which is the basic building block for multilevel inverters. The developed 2kW multilevel inverter cell is shown in Figure A-5, which only needs TTL gate signal inputs and main dc and ac bus connections. As a result, (1) no gate drive power supply is needed, (2) interconnections are minimized, and (3) compactness and high reliability can be achieved.

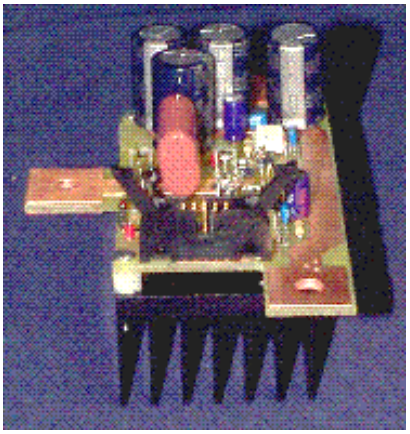

Figure A-5. 2kW multilevel inverter cell or module.

Figure A-6 shows some experimental results obtained from the 2 kW multilevel cell, where V_{GP} and V_{GN} are gate voltages and V_L and I_L are output voltage and current. A 30 kW multilevel inverter prototype using the developed multilevel cells as building blocks is been fabricated. The prototype will be tested with a motor to demonstrate the superiority.

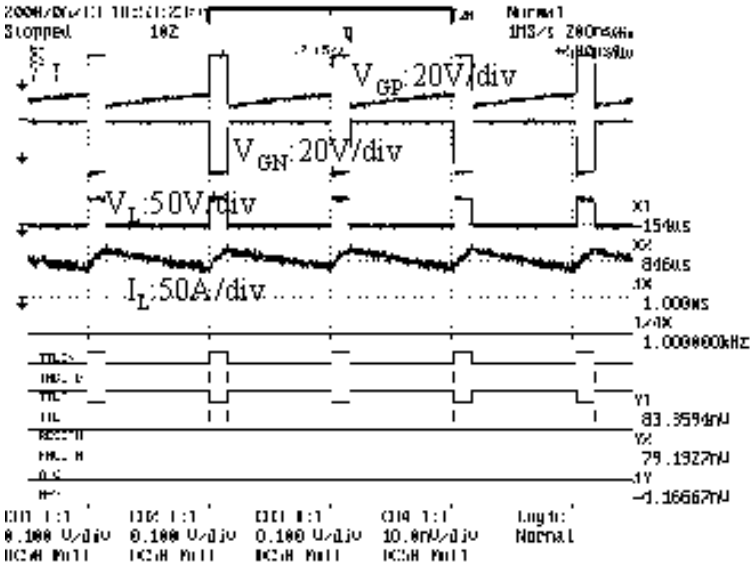

Figure A-6. Experimental results of the 2kW multilevel inverter cell.

Multilevel dc-dc Converter for Dual-Voltage Systems

Bi-directional dc-dc converters have been an obstacle for introducing 14/42 V dual-voltage systems in automotive industry. This task proposes a completely new approach to implement such dc-dc converters. Figure A-7 shows the topology of this new approach. The developed 2kW multilevel inverter cell is used as the building block. The main features of this new technology are: (1) no magnetics in the circuit, which is the troublesome component in the traditional dc-dc converters; (2) excellent manufacturability, the whole converter can be manufactured as power IC chips; (3) compact size and light weight because of no magnetics; (4) redundancy from multiple cells resulting in high reliability; (5) low cost because of use of low voltage metal oxide semiconductor type field-effect transistors (MOSFETs) and the developed self-powered multilevel cells; (6) high efficiency (~99%); and (7) low/no EMI because of low-frequency switching.

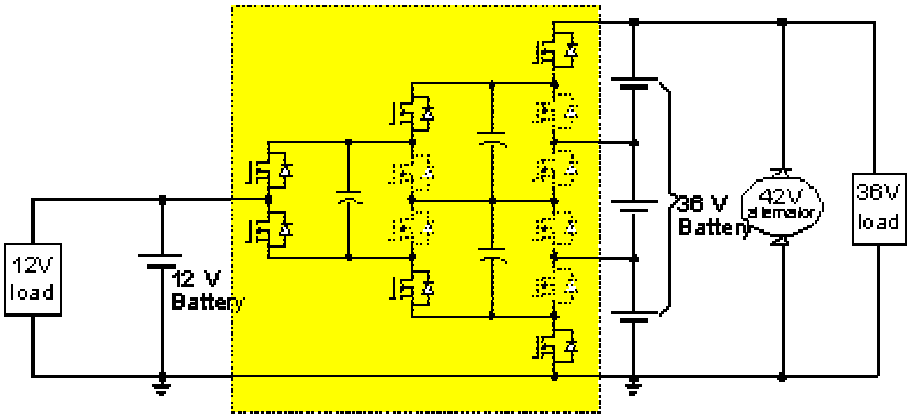

Figure A-7. A multilevel dc-dc converter for dual-voltage systems.

Simulations have been performed. Stable bi-directional power flow, well-balanced voltage levels, and easy gate control have been confirmed. A 6 kW prototype has been fabricated and is under-testing. It is believed that this new dc-dc converter technology will be widespread in such niche applications.

Publications During FY 2000

1. F. Z. Peng and D. J. Adams, "An Auxiliary Quasi-Resonant Tank Soft-Switching Inverter," IEEE IAS Annual Meeting, Rome, Italy, 2000.

2. F. Z. Peng, "A Generalized Multilevel Inverter Topology with Self Voltage Balancing," IEEE IAS Annual Meeting, Rome, Italy, 2000.

3. F. Z. Peng, "Large Motor Drives," Encyclopedia of Electrical and Electronics Engineering, John Wiley & Sons, 2000.

4. F. Z. Peng, "Compensation of Non-Periodic Reactive and Harmonic Current," IEEE Power Engineering Summer Meeting, Seattle, Washington, July 16–20, 2000.

5. F. Z. Peng, "Speed and Flux Sensorless Field Oriented Control of Induction Motors for Electric Vehicles," pp. 133–139 in IEEE/APEC, New Orleans, Louisiana, 2000.

6. F. Z. Peng, "Harmonic Sources and Filtering Approaches, -Series/Parallel, Active/Passive, and Their Combined Systems-," pp.448–455 in IEEE IAS Annual Meeting, Phoenix, Arizona, 1999.

7. L. M. Tolbert, F. Z. Peng, and T. G. Habetler "Dynamic Performance and Control of a Multilevel Universal Power Conditioner," pp.440–447 in IEEE IAS Annual Meeting, Phoenix, Arizona, 1999.

8. F. Z. Peng, et al, "A Series LC Filter for Harmonic Compensation of ac Drives," IEEE/PESC, Charleston, South Carolina, 1999.

9. J. Chang, J. Hu, and F. Z. Peng, "Modular, Pinched DC-Link and Soft Commutated Three-Level Inverter," IEEE/PESC, Charleston, South Carolina, 1999.

B. Electric Machinery R&D

John S. Hsu
Oak Ridge National Laboratory
National Transportation Research Center
2360 Cherahala Boulevard
Knoxville, Tennessee 37932
Voice: 865-946-1325; Fax: 865-946-1210; hsujs@ornl.gov

Objectives

The objectives of the electric machinery R&D project for the HEV motors are:

- Reduce cost and weight,
- Improve performance,
- Simplify system, and
- Increase reliability.

Approach

- In order not to miss an important task, the project initially investigates technologies with a relatively wide scope.
- Prioritize tasks after reviewing the initial investigation.
- Pursue cooperation with industry.

Accomplishments

- Six patents have been granted to the Laboratory through this project.
- Prototypes of several tasks are built and tested during the initial wide-scope investigation.
- A major automotive supplier and an original equipment manufacturer (OEM) are interested in the copper-rotor and slot-utilization technologies developed through this program.

Future Direction

- Work closely with industry to use the technologies.
- Further prioritize the tasks to meet the budget limitation.

Introduction

The PNGV 2004 cost and weight goals for electric machinery are $4/kW and 2kW/kg; and for inverter are $7/kW and 5kW/kg. The total cost target for both electric machinery and inverter is $11/kW. Having these goals in mind, four groups of machines and technologies are initialized and investigated under different priorities. The first group is the unconventional approach that includes: the soft commutated dc machines, brush technology, winding insulation of conductors, and the high-power-density homopolar motors. The second group is the manufacturing

technology of copper rotors and the slot fill improvement for induction motors. The third group is the permanent magnet (PM) machines that comprise the directly controlled field weakening of PM machines and the flux guides for PM machines. The fourth group is the switched reluctance motors (SRMs). Six patents were granted to the laboratory during the wide-scope investigation.

The project currently focuses on the soft commutated dc motor, the advanced brushes, and the copper-bar rotor tasks that show significant potential for cost reduction.

Soft Commutated DC Machines
(U. S. Patent 5,929,579)

There is no doubt that a low voltage motor drive system increases consumer safety and lowers liability cost. A 24V (i.e., 34V peak) ac voltage is commonly used for the home central air conditioning control. The general practice among industry in the United States normally allows one person working on a job at a voltage below 50V. Two trained electricians must be assigned for a job at a voltage between 50V and 600V. The safety versus voltage is an important issue for the HEV program. From the inverter standpoint, a low voltage drive system may be inefficient due to the approximate 2.5V drop on a typical IGBT. For each phase that goes through, two IGBTs may have a 5V drop. This voltage drop is a direct loss and becomes significant when the system voltage is low. For example, if the system voltage is 42V. The percentage of 5V/42V=11.9% is the conduction loss of the IGBTs.

This project shows that the soft commutated dc motor can be built for a low voltage. The system voltage for a 55 kW prototype motor may be as low as 13V. This can only be achieved through our advanced brush that has a very low voltage drop. A dc motor can run directly from a dc supply without an inverter, it simplifies the system and provides possible savings from eliminating a full-rating dc/dc converter and a full-rating inverter.

Figure B-1 shows the potential schematic diagram of a targeted system. The output voltage of the fuel cell is controlled directly by the driver's foot paddle. More fuel goes into the reformer and higher voltage of the fuel cell goes out to the soft commutated dc motor directly.

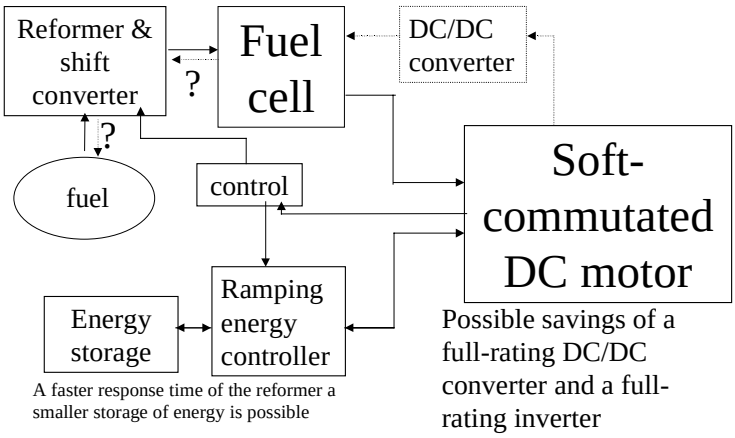

Figure B-1. A schematic diagram of a targeted system.

It is certain that the response time of the fuel cell voltage output cannot follow the fuel input right away. A ramping energy controller, which energy rating goes down when the responsive time becomes shorter, is definitely needed. As the fuel cell technology develops, this responsive time becomes shorter.

A motor can be overloaded five or six times its rating for a short period of time without damaging the motor. It is obvious to see the advantages of the targeted system of Figure B-1 from the standpoint of its low drive system cost, no need for inverter, high overload capability, and robustness of the system. The common concern is the use of brushes in an electric machine. The following achievement of our advanced brush and lubricant may help to ease this concern.

Before introducing our advanced brush, we may want to look at the reality of the market. There is no doubt that a sliding brush in a motor would have a shorter life expectancy than a motor without any sliding brush. Changing the brushes after a certain time period may be required. For a consumer product, a longer life expectance with higher price may not be what the consumer wants. For example, a typical washing machine's life expectancy is designed to be about five years. However, one can increase its life expectancy by changing all the steel components to stainless steel except the motor to prevent rusting. It is engineering feasible, but it would cost more and may not be what most consumers need. There is always room for a deluxe product. Similarly, the consumers may accept a simple system having our advanced brushes and soft commutated dc motor with a reasonable life expectancy for minimizing the frequency of brush replacement to address the lower cost demand.

Advanced Brush Technology

Figure B-2 shows the comparison of the voltage drops between our (i.e., ORNL) new brush and the best commercially available graphite brush. Our brush can carry three to four times the current of the graphite brushes and has less than one-volt drop across the two brushes. The lubricant helps to reduce the wear and tear of the commutator and brushes.

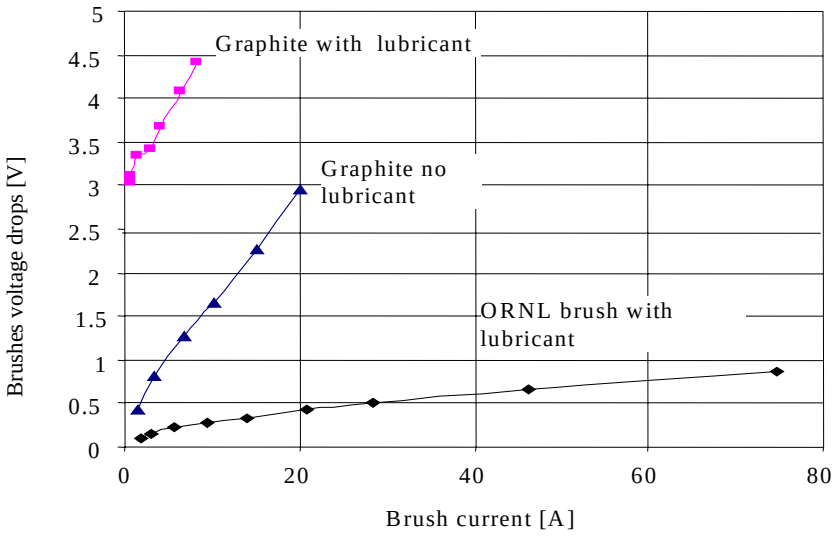

Figure B-2. A schematic diagram of a targeted system.

Unlike the graphite brushes, the brush voltage drop of our advanced brush is extremely low at the low current region. This means that the efficiency of the motor is high at low load when using our advanced brush. This is also an advantage over the IGBT, and is similar to the trend of a MOSFET's voltage drop.

Figure B-3 shows the brush voltage drops of our advanced brush under various operating conditions. The lubricant does not post any practical harm to the brush voltage drop.

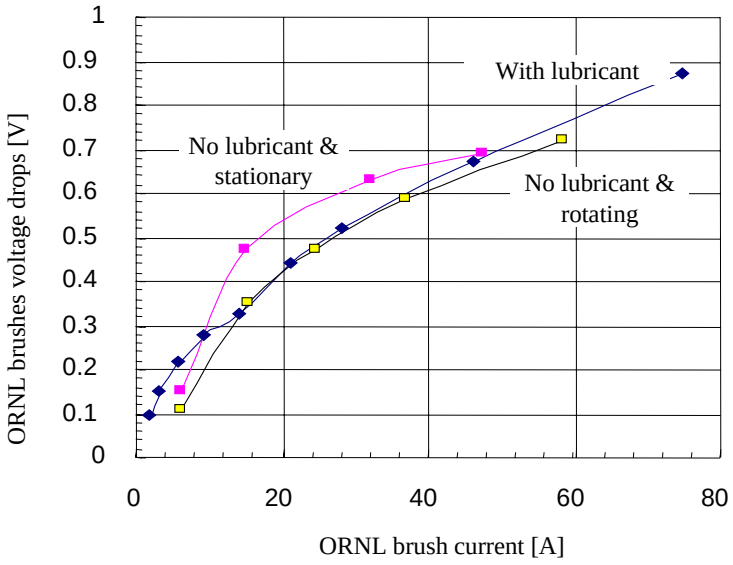

Figure B-3. Brush voltage drops of ORNL brush.

Figures B-4a-e shows traces of voltage drops across the two brushes. Figure B-4a is for the graphite brushes carrying 23 amperes without lubricant at the stationary mode. The voltage drop is around 1.8V. Figure B-4b corresponds to the graphite brushes carrying 20 amperes without lubricant at the rotating mode. The voltage drop is around 3V. Figures B-4c and B-4d are for the graphite brushes carrying 9 amperes with lubricant at the rotating mode. The brush voltage drop is higher than 3 volts. The spikes shown in Figure B-4d indicate that occasionally the graphite brushes are chattering. Figure B-4e is for our advanced brush carrying a remarkable 75 amperes with lubricant at the rotating mode. The voltage drop is around 0.9V. The voltage drop goes down at lower current. In short, the significant property of our advanced brush is the greater than three times of the current carrying capability (75A versus 20A) and with a less than one third of the graphite brush voltage drop.

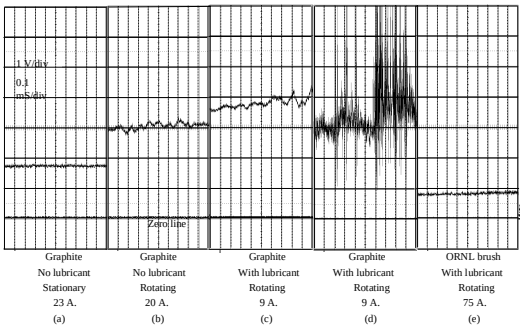

Figure B-4a-e. Comparison of traces of various brush voltage drops.

Another important development for increasing the life expectancy of our brushes and commutator is to suppress the sparks through the soft commutation. The principle of the soft commutation is to drain the current of a coil before the coil is disconnected from its current path. It can be explained through Figure B-5.

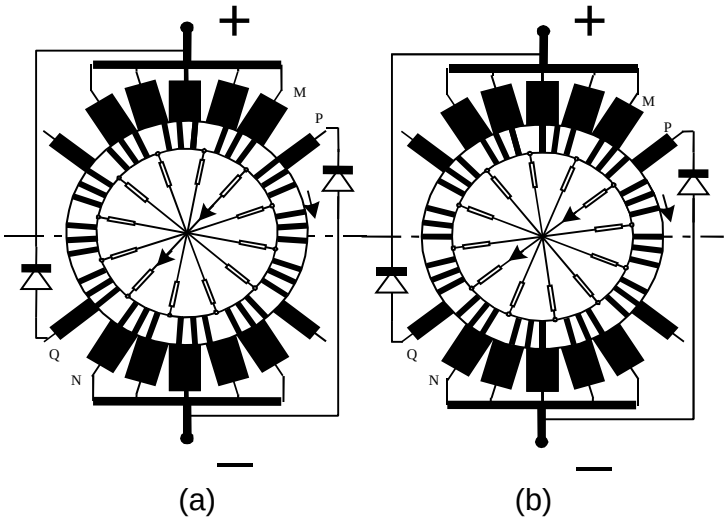

Figure B-5. Principle of soft commutation.

Figure B-5a shows the power supply terminals, + and -, the main brushes connected in parallel to the power supply, and the small commutating brushes. The ring with segments represents the commutator having the large segments made of conducting material and the small segments made of insulating material. The armature coils are represented by the components inside the commutator. The coil leads are connected to the opposite large commutator segments. The coil current goes through the main brush, M, the commutator large segment, the coil marked with arrows, the opposite large commutator segment, the main brush, N, and returns to the negative terminal of the source. When the said large segments are about to leave the brushes, M and N, the commutating brushes, P and Q, are making contacts with the said coil. Figure B-5b shows that the current in the said coil can drain through the diodes connected to the commutating

brushes, P and Q, back to the power supply. The energy stored in the said coil is totally drained before leaving the commutating brushes.

Figure B-6 shows a 25kW prototype of the soft commutated dc motor. The section in white color is the housing for the brushes.

Figure B-6. A 25kW, 13V, 4500A soft-commutated dc prototype motor.

The structure of the prototype rotor shown in Figure B-7 is very simple. The winding is like a rotor cage of an induction motor. An end ring is shown on the right-hand side. The rotor bars extend toward the left-hand side and form a commutator. The center ring is a band on the rotor bars to increase the rotor strength for withstanding the centrifugal force.

Figure B-7. Rotor of the soft-commutated dc prototype motor.

Winding (Bar) Insulation

Figure B-8 shows the ceramic coating applied to the copper surface through the plasma spray. This insulation can withstand high temperature and provides an extremely high overload capability. The rotor is robust and the low operating voltage also helps to improve the reliability of the motor.

Figure B-8. Plasma spray for bar insulation.

Progress in Copper Rotor Task

Figure B-9 shows a 1000X view of a faultless joint of the copper bar and aluminum end ring.

We are currently working on the improvement of manufacturing fixtures for the rotor punching stacks that use our technology.

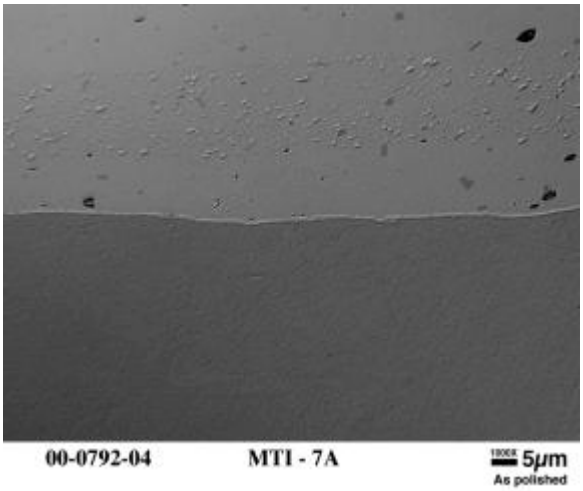

Figure B-9. A 1000X view of a faultless copper/aluminum joint.

Conclusions

The goal of this project is to meet the Department of Energy's (DOE's) objectives for lowering the cost of electric machinery and its related drives for HEV applications. A major automotive supplier and an OEM are interested in our copper bar and slot utilization technologies. We shall pursue further cooperation with industry for the technologies developed under this task.

Our soft commutated dc motor and the advanced brush tasks address an unconventional approach that has a tremendous potential to lower cost, improve efficiency, increase consumer safety, and simplify system.

References

1. John S. Hsu, "A Machine Approach for Field Weakening of Permanent-Magnet Motors," 2000 Future Car Congress, Paper No. 2000-01-1549, *Society of Automotive Engineers*, April 2–6, 2000.

2. John S. Hsu, "Direct Control of Air Gap Flux in Permanent Magnet Machines," Paper No. TR7001, 2000, *IEEE Transactions on Energy Conversions*.

3. John S. Hsu, "Soft Commutated Direct-Current Motors," 1998 IEEE Workshop on Power Electronics in Transportation, IEEE Power Electronics Society, Dearborn, Michigan, October 22–23, 1998.

4. John S. Hsu, *Direct Control of Air Gap Flux in Permanent Magnet Machines*, U.S. Patent No. 6,057,622; May 2, 2000.

5. John S. Hsu, *Permanent Magnet Energy Conversion Machine*, U.S. Patent 5,952,756; September 14, 1999.

6. John S. Hsu, *Soft-Commutated Direct Current Motor*, U.S. Patent No. 5,929,579; July 27, 1999.

7. John S. Hsu, *Method and Apparatus for Assembling Permanent Magnet Rotors*, U.S. Patent No. 5,914,552; June 22, 1999.

8. John S. Hsu, *Extended Cage Adjustable Speed Electric Motors and Drive Packages*, U.S. Patent No. 5,886,445; March 23, 1999.

9. John S. Hsu, *Homopolar Motor with Dual Rotors*, U.S. Patent No. 5,844,345; December 1, 1998.

C. Field Weakening and Magnet Retention for PM Machines

John W. McKeever
Oak Ridge National Laboratory
National Transportation Research Center
2360 Cherahala Boulevard
Knoxville, Tennessee 37932
Voice:865-946-1316; Fax 865-946-1210; mckeeverjw@ornl.gov

Objectives

- Analyze known field-weakening methods for electronically switched PM type motors and identify deficiencies that may limit their use as an HEV drive system.
- Where possible, correct limiting deficiencies to produce a controller that is able to drive PM motors above base speed.
- Build and test a PM motor/controller system that can deliver constant torque to base speed and 15 kW power from base speed to 4.5X base speed.
- Compare attributes of all PM type motors that are PNGV HEV candidates and recommend one as the PM traction motor system of choice.

Approach

- Classify and study PM motors suitable for PNGV application by the shape of their back-emf, which is sinusoidal for PM Synchronous Machines (PMSMs) and trapezoidal for brushless dc machines (BDCMs) – 1999.
- Explore their ability to be driven above base speed, which is the speed where back-emf equals the bus voltage, to identify limiting deficiencies – 1999.
- Complete and publish theoretical development of the new Dual Mode Inverter Control (DMIC) method, which enables BDCMs to deliver constant power above base speed without exceeding current rating at base speed – 2000.
- Demonstrate the DMIC in the laboratory driving a derated PM axial-gap motor – 2000.
- Demonstrate a DMIC specifically designed and integrated to drive a 15 kW PM axial-gap gearless HEV traction motor – 2001.

Accomplishments

- Submitted a patent application for the DMIC, which is able to drive PMSMs and BDCMs to 6X base speed as either a motor or generator without exceeding the rated base speed current.
- Drove a PM axial-gap motor, which was derated to deliver 7.5 hp at a base speed of 400 rpm, using the first DMIC controller to 2424 rpm without exceeding the base speed current.
- Completed *Extended Constant power Speed Range of the Brushless dc Motor through Dual Mode Inverter Control,* ORNL/TM-2000/130, June 2000.
- Completed the initial design of the 15 kW axial-gap PM traction motor and the DMIC with which it will be integrated as a PNGV HEV candidate.

Future Direction

- Complete the design and build the 700 rpm base speed axial-gap PM motor that can continuously deliver 15 kW – 2001.
- Complete the design, build, and integrate the DMIC with a speed control loop – 2001.
- Optimize the DMIC topology with respect to system voltage drops, part count, and efficiency – 2001.
- Optimize the control system and complete a performance test – 2001.
- Analyze the performance of the new switching control technique – 2001
  - for a PM motor with sinusoidal back-emf (up to this point the demonstration motors have had trapezoidal back-emf).
  - for a switched reluctance motor.
- Recommend the PM traction drive system (SRM, PMSM, or BDCM) that has best performance with respect to HEV constraints – 2002.
- Build or obtain the PM traction drive system and characterize it in the laboratory – 2002.

Introduction

Because of their inherent high-power density and efficiency, BDCMs with surface mounted rare-earth PMs can provide the traction drive system needed by HEVs. Until now there has not been a practical way to drive these motors over a constant power speed ratio (CPSR) of 5:1 or more. Today's technology for driving above base speed is the phase advance method (U.S. Patent Number 5,677,605 – October 14, 1997). Although it can control the motor power over such a speed range, the current at high speed may be several times greater than that required at base speed. The increase in current during high-speed operation is due to the low motor inductance and the action of the bypass diodes of the inverter. The use of such a control requires increased current rating of the inverter semiconductors and additional cooling for the inverter and the motor.

This limitation of the Phase Advance Method led to the discovery of a new inverter topology and control scheme, which can drive a low-inductance BCDM over the CPSR required in electric vehicle applications. The controller is called the DMIC. There is no theoretical limit to its CPSR if hysteresis, eddy current, and semiconductor switching losses are ignored. Lab experience demonstrated delivery of 7.5 hp at a CPSR of 6 without exceeding the rated current at base speed.

The DMIC has the following features:

1. The DMIC provides the functional equivalent of field weakening without requiring an auxiliary field winding or rotor saliency.
2. The DMIC works well with low inductance motors (i.e., rare-earth PMs) preserving their high power density.
3. Motor current does not exceed base speed current over extended CPSRs.
4. Motoring and regeneration are possible. It is possible to generate at many times rated power for brief periods making this control method attractive for applications requiring rapid regenerative braking.

5. In battery-driven applications, the controller functions over a wide range of battery voltages.
6. The controller works well with non-salient rotor designs. Interior-mounted PMs are not required.
7. The motor back-emf can be sinusoidal as well as trapezoidal.
8. The inverter is capable of extinguishing the motor current within 1/6 to 1/2 of a fundamental cycle if a fault develops in the dc supply system.
9. Usual methods such as sinusoidal PWM for sinusoidal back-emf motors and hysteresis band current control for trapezoidal back-emf motors may be used for operation below base speed. Operation above base speed involves switching at the fundamental frequency that eliminates high-frequency switching losses.
10. Controller calculations are not elaborate and may be implemented with a digital signal processor (DSP) or a small microprocessor.

Theoretical

Report ORNL/TM-2000/130 quantitatively explains how the DMIC method controls operation of the BCDM above base speed. Calculations are based on parameters for a low-inductance axial gap BDCM designed and built by ORNL and show how the phase advance method compares with the DMIC method for constant power operation above base speed.

The primary problem with the phase advance method for operation of low inductance motors above a CPSR of 2 was the uncontrolled conduction of the inverter bypass diodes. For example, for 36 kW total power, the average power through each phase must be 12 kW. For the phase advance method, this 12 kW consisted of 71.6 kW of motoring power through the semiconductor and 59.5 kW of regenerated power back through the bypass diode. The DMIC avoids this by using an inverter topology different than that of the common voltage fed inverter. Figure C-1 compares the two topologies. By appropriate control of the thyristors, the detrimental mixture of motoring and generation can be avoided during routine operation in the motoring mode.

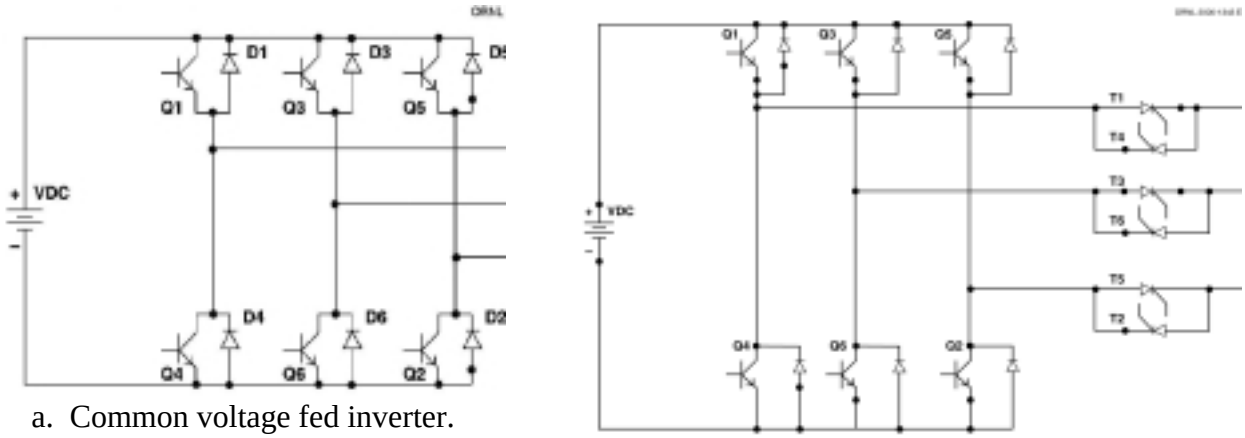

a. Common voltage fed inverter.

b. New DMIC topology.

Figure C-1. Comparison of the voltage fed and dual mode inverter topologies.

Theoretical expressions for average power, peak current, and root mean square (rms) current show that the output power is linearly dependent on the supply voltage and that, if the supply voltage is reduced, the desired power may be restored by increasing the advance angle. Increasing the advance angle increases the motor current. Results from a PSPICE simulation compare well with the theoretical results and with a lab demonstration to confirm that the DMIC offers a substantial increase in the CPSR performance of the BDCM.

Experimental

The DMIC was fabricated to drive an ORNL axial gap BDCM derated to 7.5 hp at a base speed of 400 rpm. Its silicon controlled rectifiers (SCRs) were controlled by a modification of the algorithm in the digital signal processor that operates ORNL's pseudo PWM drive inverter. The test configuration is shown in Figure C-2. The test setup is shown in Figure C-3. Results of the test are shown in Figure C-4. The results confirm that over a CPSR of 6 the current maintains its base speed value while the motoring power is at least as high as the power delivered at base speed.

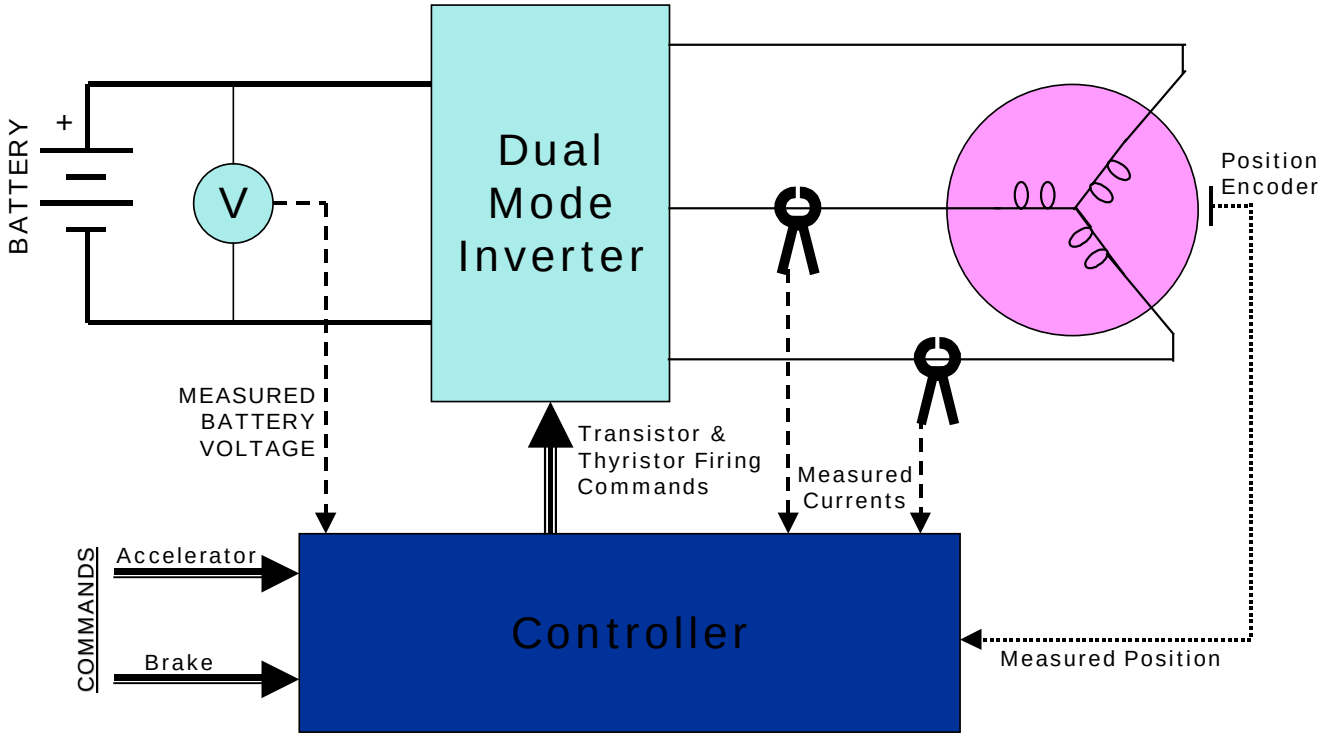

Figure C-2. Configuration of DMIC verification test.

Figure C-3. DMIC verification test setup.

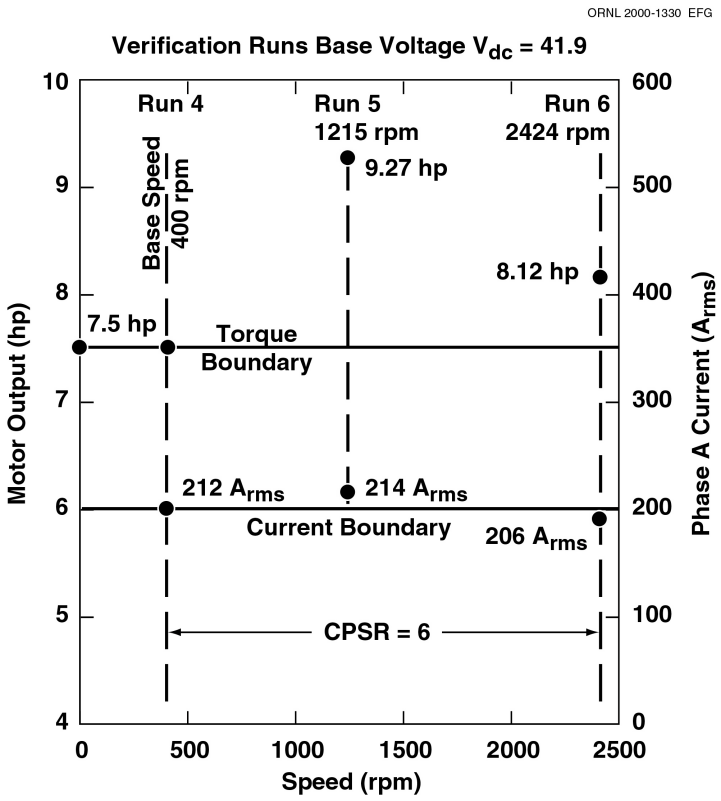

Figure C-4. Results of DMIC verification test.

Design of Integrated HEV Traction System

A preliminary design of a 15 kW HEV traction system has been completed. Construction of the BDCM has begun. Figure C-5 shows an exploded view of the new BDCM design. Fabrication of the DMIC will provide more information about the actual cost and size.

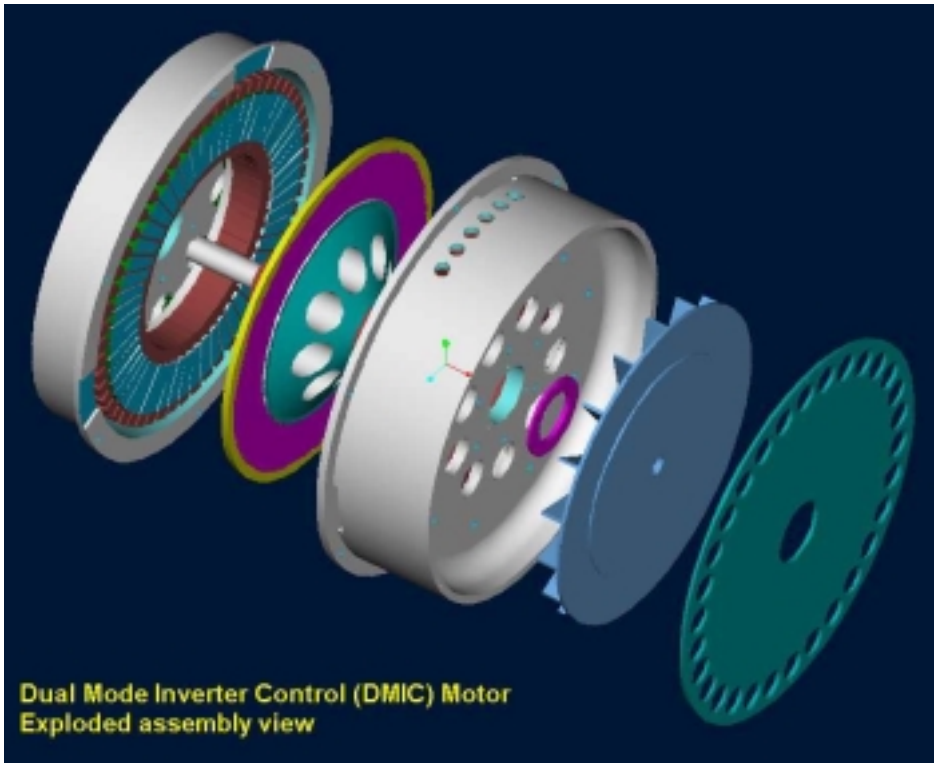

Figure C-5. Exploded view of the 15 kW axial-gap HEV traction motor.

Conclusions

Theoretically, the BDCM has been shown to have an infinite CPSR when driven by the DMIC providing a practical way to drive a BDCM up to six times base speed.

Essentially the effect of field weakening is achieved without interior-mounted magnets or supplementary field windings. The rms current in the constant power range is no greater than the rms current required to produce full power at base speed allowing cost, weight, and volume optimization of motor design at base. These features should make the BDCM a viable alternative for HEV traction applications. In addition to extending the constant power range, it can improve electrical safety by preventing the motor from feeding faults that might develop in the dc supply system for more than 1/6 to 1/2 of a fundamental cycle.

Demonstration of an HEV traction system that incorporates the DMIC is planned for FY 2001.

References/Publications

J. M. Bailey et al., *Field-Weakening Schemes and Magnet-Retention Techniques for Permanent Magnet Machines,* ORNL/TM-1994/74 (draft), Oak Ridge National Laboratory, Lockheed Martin Energy Research Corporation, 1999.

J. S. Lawler and J. M. Bailey, *Constant Power Speed Range Extension of Surface Mounted Permanent Magnet Motors,* Disclosure ERID 0716 : Patent Application submitted, 2000.

J. W. Lawler, J. M. Bailey, and J. W. McKeever, *Extended Constant Power Speed Range of the Brushless DC Motor through Dual Mode Inverter Control,* ORNL/TM-2000/130, Lockheed Martin Energy Research Corporation, June 2000.

D. Microsensors for Automotive Power Electronics

Stephen W. Allison
Oak Ridge National Laboratory
National Transportation Research Center
2360 Cherahala Boulevard
Knoxville, Tennessee 37932
Voice: 865-946-1287; Fax: 865-946-1210; allisonsw@ornl.gov

Objectives

- The purpose of this project is to develop an economical voltage and current sensor with improved performance for the hybrid electric vehicle power electronics package. The approach makes use of fiberoptics and microelectromechanical systems (MEMS) technology. Specifically, microcantilevers coated with magnetic material are the sensing elements. They flex in the presence of a magnetic field that is induced by current in a conductor. This flexure of a few nanometers in amplitude is detected optically.

- The impetus behind this effort is that this approach has the potential to reduce cost, weight, and volume necessary to perform the required diagnostics for the inverter. In addition, the approach should be more power efficient.

Approach

The physical basis for this project is the fact that any current carrying conductor will generate an associated magnetic field. This magnetic field can be described in terms of Ampere's Law:

$$\circ B \bullet dl = \mu oi \, .$$

As an example, for the elementary case of a long straight wire, this equation can be used to show that the induced magnetic field is a simple relation:

$$B = \frac{\mu oi}{2\pi r} \, .$$

Therefore, a sensitive and responsive device that can measure a magnetic field at a fixed distance from a conductor is also sensing current.

Figure D-1 shows how the magnetic field decreases as a function of distance from a conductor based on the above equation for several currents. To summarize, if a sensor is placed within a millimeter of the conductor, the field exceeds at least several Gauss.

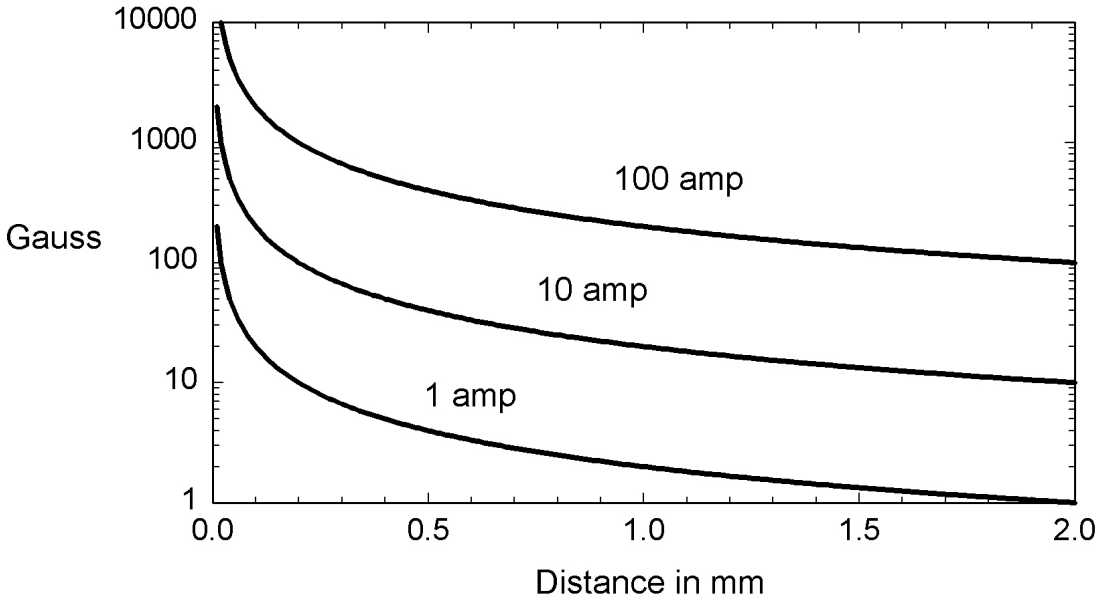

Figure D-1. Magnetic field vs distance from a current source for 1, 10, and 100 amps.

Such fields are sufficient to produce flexure of the MEMS sensors tested here. Figure D-2 illustrates a sensor configuration.

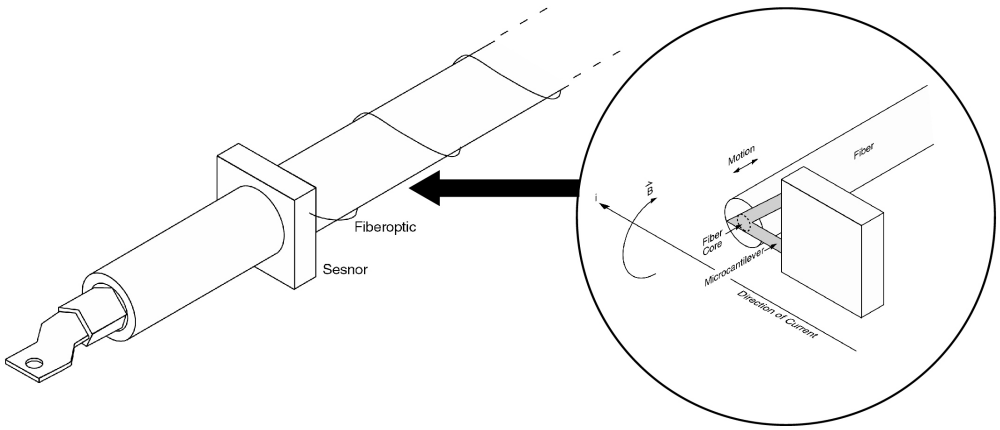

Figure D-2. Sensor arrangement.

The target specifications are as follows.

Characteristics	Performance Limits
Size	< 10 cm^3
Cost	$1 to $5
Weight	50 g
Temperature	-40 to 150 C
Humidity	0 to 100 RH
Vibration (3 to 200 Hz)	10 g

Accomplishments

1. Improved Magnetic Materials Deposited and Tested

Whereas in the first year of the project, cantilevers were coated with one magnetic material, iron. This material degraded in time due to rusting thus decreasing the responsiveness to magnetic fields. It was found that this could be solved, at least in part, by an additional coating step. This was the depositon of a passivation layer of platinum. However, in this past year two superior coatings were demonstrated that exhibited higher sensitivity and no discernible degradation. No extra coating step was required. The two materials are:

- cobalt
- permalloy.

2. Coating Methodology

Ion beam sputtering and pulsed laser deposition are two methods for depositing magnetic material on cantilevers. Both techniques have their respective advantages. The simplest and cheapest to operate is ion beam sputtering. Thus steps were taken to improve it. One drawback had been that the sputtering system could only coat one side of a cantilever at a time. The sputtered ions are hot and this sometimes caused the coated cantilever to warp. To overcome this, the apparatus was modified to rotate the sample so that both sides of the sample are coated. With this additional sample preparation procedure, the warping problem is essentially solved.

3. Time Response

To demonstrate time response capability, a 10 kHz oscillating current was directed to a Helmholtz coil. This cobalt-coated microcantilever was in the center of the coil field. The field fluctuations were only a few Gauss. It is seen in Figure D-3 that the sensor's cantilever deflection does follow the sinusoidally varying magnetic field and hence current. Subsequent tests have attained 50 kHz. Mechanical modeling indicates that a 1 MHz response is attainable and realistic.

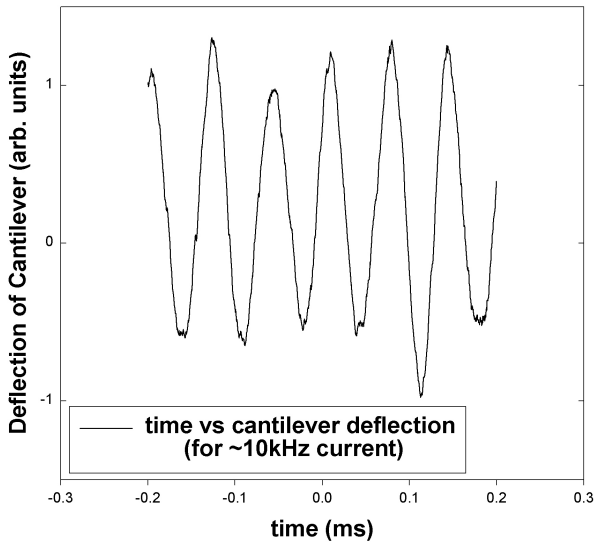

Figure D-3. Deflection of microcantilever produced by current oscillating at ~10 kHz.

4. Sensitivity versus Frequency

The cantilevers are mechanical structures with a characteristic resonant frequency. At that frequency they are more sensitive to current. This is illustrated below for two different sensors of permalloy and cobalt in Figures D4 and D5, respectively. This resonant frequency is adjusted by changing the dimensions of the cantilever and coating thickness. For these tests, a lock-in detector is used and its output represents the maximum amplitude of the swing of the cantilever. Even though the signal is weaker to the low frequency side of the resonant frequency, in general it is still detectable.

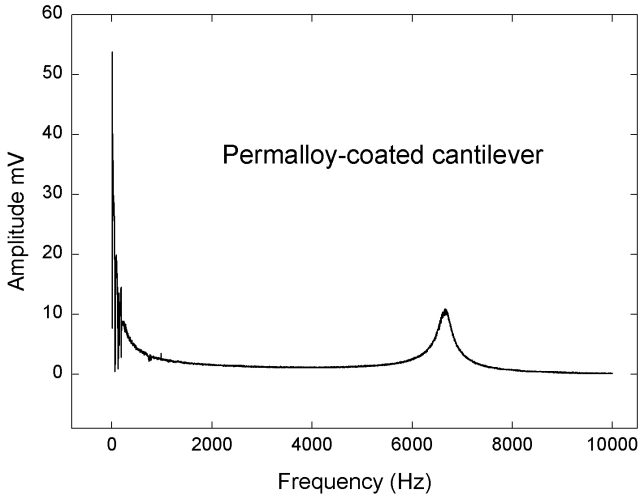

Figure D-4. Response of permalloy-coated cantilever as a function of frequency.

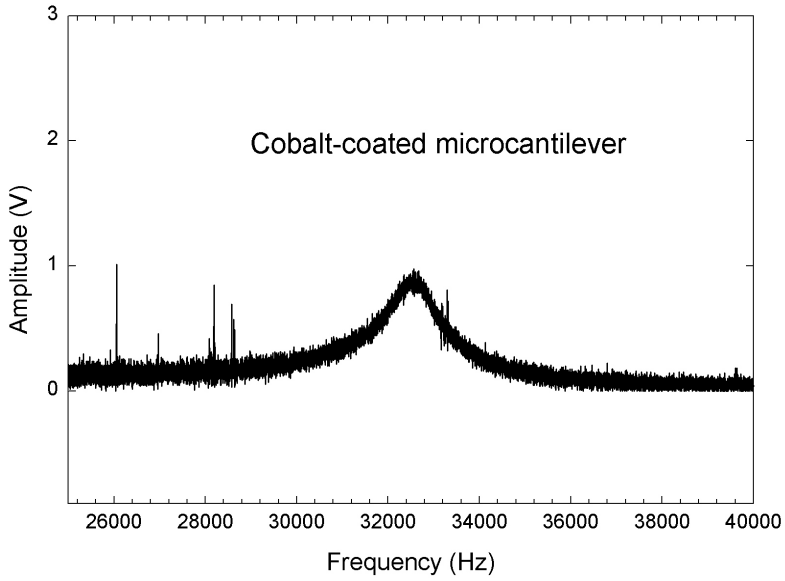

Figure D-5. Response of cobalt-coated cantilever as a function of frequency.

Summary

In summary, two coatings not subject to corrosion were demonstrated. Modification of the ion deposition device yielded higher quality coating without warping the cantilever. Tests showed that the motion of the cantilever does follow the dependence of the magnetic field and current for signals varying as rapidly as 50 kHz.

Future Directions

Tests are underway to identify the role of coating thickness and cantilever dimensions with respect to sensitivity and time response. The effect of masking off and thus coating only a portion of the cantilever is being explored as it may give greater flexibility in sensor design. In addition, the fiberoptic arrangement for measuring cantilever flexure is being miniaturized. Future plans are to demonstrate a prototype similar to the depiction of Figure D-2. Extended tests will be performed in an inverter and a high vibration environment. The overall goal is to achieve the appropriate performance using methods and components that will, with the expected economy of scale, result in inexpensive yet high performance devices.

Publications

S. Goedeke, "A Novel MEMS-Based Magnetic Field Sensor," (in preparation) to be submitted to *The Review of Scientific Instruments.*

E. Automotive Integrated Power Module (AIPM) Validation Testing and Contract Support

Curtis W. Ayers
Oak Ridge National Laboratory
National Transportation Research Center
2360 Cherahala Boulevard
Knoxville, Tennessee 37932
Voice: 865-946-1342; Fax: 865-946-1210; ayerscw@ornl.gov

Objectives

- The goal is to provide technical support to the AIPM Contracts Manager to develop test procedures, design, acquire and prepare the test equipment, and to perform the validation testing of the AIPMs supplied by DOE's AIPM contractors.
- To provide electrical and environmental test support to AIPM developers/suppliers of preliminary and production design AIPM test articles leading to the refinement of the deliverable units. The conformance to established specifications will be assessed and the results will be utilized to determine the suitability of the AIPM technology for automotive applications.

Approach

The AIPM validation and test support effort will be accomplished through the development of validation criteria taken from test data requirements set forth in industrial standards. Necessary test documents and standards will be acquired and studied in order to develop comprehensive testing protocols. Pass/fail criteria will evolve into electrical and environmental test procedures for qualifying the units. Drafts of the procedures will be reviewed by Electrical and Electronics Technical Team (EE/TT) members and in-house testing staff. Acquisition and/or fabrication of equipment necessary to accomplish the testing tasks will be performed and scheduling of the tests, test facilities, and necessary personnel will be coordinated. Efforts will be made to minimize expenses and provide the most expedient results in the validation process through the utilization of ORNL in-house expertise and equipment.

Accomplishments

- ORNL is tasked with the evaluation of three vendors' power modules designed for automobile traction motor drives. These evaluations will include basic electrical/electronic functionality testing followed by load and control testing driving a standard motor. Environmental tests will follow the functional and load tests. This segment of evaluations includes thermal cycling and soak, salt spray, dust infiltration, vibration shaker, and shock tests. Electromagnetic emissions will be measured when the units are at various load conditions on the test stand.

- Referenced test standards and pertinent documents have been acquired and studied. The selections of valid tests and test sequencing of the modules was finalized. Questions concerning the AIPM specification and solicitation involving current and power levels as well as specific environmental tests were addressed. The effected documents were amended and submitted to DOE. Recommended changes to the AIPM specifications have been submitted to the program participants.

- The environmental test procedures were completed and reviewed by subject matter experts. The development of the functional test and electrical characterization tests are nearly complete. The report template, which will accompany the test unit throughout its testing cycle, is being written. Upon completion of the electrical tests, a testing flowchart will be created that will be included in the test documentation package. The flow chart will contain test decision points and branches. This will be available to the test operator throughout testing to insure consistent, adequate, and thorough evaluation of the modules.

- The purchase or design of equipment necessary for the testing of the AIPMs is nearly complete. All test equipment that will be procured during FY 2000 has been placed on order and equipment is arriving on site. Computers and data acquisition equipment to allow for monitoring of testing via the Internet have arrived as well as numerous meters and other electrical support equipment. Current sensors, power supplies, and motors for load simulation are due in before the end of the fiscal year. Some upgrades of the environmental test equipment have been made.

- A design for a relatively small, inexpensive cooling system for the AIPMs has been completed and parts have been procured. Parts for the second power supply have been obtained and the build of this unit is complete. Test equipment has been acquired.

- Arrangements and plans to provide for all testing to be conducted at ORNL have been finalized. Economical means have been devised to enable the performance of dust tests to be done on site rather than going to a commercial test laboratory. Designs for these alternative test facilities have been reviewed. All support equipment necessary for the tests have been identified.

- The PEEMRC is relocating to the NTRC and the dynamometer is to be assembled with data acquisition hardware and software specifically for testing AIPMs. The software will be developed to allow automatic and possibly remote control of the testing and data acquisition. The dynamometer will be controlled by computer allowing long term tests with automatic data acquisition, as well as variable load cycles (such as the Federal Urban Driving Schedule (FUDS) to simulate real world loads on the motor/AIPM.

Future Direction

- In FY 2001, the detailed test plans for the evaluation and validation of the AIPM will be finalized. Continuing issues and comments received from the EE/TT and vendors about the test requirements for the AIPM units will be addressed/resolved. The prototypes are expected at ORNL in the fourth quarter of FY 2001 or the first quarter of FY 2002. PEEMRC will

finalize the development of the dynamometer control concepts and data acquisition methods that will be required for the evaluating the AIPMs.

- After installation of the new dynamometer, testing scenarios will be developed and tested using a standard inverter with a standard load motor to insure end-to-end completeness of the testing procedures. Loading algorithms and automated data acquisition programs will be tested and finalized in this manner before receipt and testing of the vendors' prototypes begins.

F. HEV Motor/Inverter Modeling

John W. McKeever
National Transportation Research Center
2360 Cherahala Blvd.
Knoxville, Tennessee 37932
Voice:865-946-1316; Fax 865-946-1210; mckeeverjw@ornl.gov

Objectives

- Develop application independent physics-based models for PM motors, induction motors, and SRMs which, along with their semiconductor based inverters, are candidates for HEV motor/drive systems.
- Develop environmental interaction models to interface these HEV motor/drive models with their surroundings and with ancillary components such as batteries, regenerative brakes, etc.

Approach

Models are constructed using LabVIEW's Application Builder and provided as a user-interactive file containing performance evaluation modules that can be run independently or in conjunction with the design modules.

The PM motor design tool has the following seven modules:

- Design module for parametric studies and optimization.
- Performance curve module coupled to the design module.
- Driving cycle evaluation module (FUDS, FHDS, NYCTruck,…) coupled to the design module.
- Drawing module for rotor/stator visualization and construction.
- Control module for study of the motor's time response to variations in load and motor inertia.
- Road test module for study of motor's time response to variations in speed, load, and ambient temperature.
- Performance map module to generate files that may be used by DOE's detailed HEV simulation codes.

FY 2000 Accomplishments

- Extended the Radial Gap Permanent Magnet (RGPM) motor design model to provide driving cycle efficiency data during the design process. Six city and country driving schedules were added to the cycle evaluation database.
- Extended the driving cycle evaluation module to allow assessment of (1) the impact of gear-ratio selection; (2) cycle statistics; (3) regenerative operation, and (4) hybrid configuration in which the user can select a power level at which the electric drive will engage. Below this level we assume the power is supplied by an internal combustion engine (ICE).

- Collaborated with representatives from industry and DOE headquarters and labs to define that the ORNL models will support DOE full vehicle simulation codes by generating importable maps.
- Extended the RGPM motor and drive model to produce maps for direct use by the full vehicle code, ADVISOR.
- Received approval from DOE to assert copyright on the RGPM model so that it may be distributed to the HEV community.
- Prepared and delivered paper 00FCC-36 "Model-based Generation of Scaling Laws for Radial-Gap Permanent Magnet Motors," at the Future Car Congress using the RGPM code.
- Completed a no frills axial-gap PM motor model with either one or two stators.
- Completed the first stage of development of the switched reluctance interactive motor model.

Future Direction

- Continue development of the switched reluctance drive system and obtain DOE approval to assert copyright so that it may be distributed.
- Document the models that have been completed.
- Facilitate an efficient method of distribution and support.
- Affirm models with experimental data. Test data supplied by Argonne National Laboratory will be compared to computations from the RGPM model.
- Apply models to expose drive system deficiencies and to provide solutions for those deficiencies.
- Add a "database" feature that stores materials and designs entered by the user for subsequent analysis.
- Adapt model development to evolving needs of HEV drive systems.
- Refine existing models to enhance their usefulness to HEV developers.

Introduction

Computer simulations are critical during design and evaluation of new technologies competing for implementation as consumer products. ORNL views as essential the development of user friendly tools, which are based on first principles, for simulation of electric motors and drives to guide configuration of electric vehicles and hybrids. Under the auspices of the U.S. DOE's Office of Advanced Automotive Technologies (OAAT), ORNL is developing tools to evaluate performance and to formulate scaling algorithms for induction, PM, and reluctance motors regarding efficiency, weight, cost, and requirements. These tools will be copyrighted by DOE and distributed freely to the automotive community.

Approach for Model Development

Fundamental mathematical-physical principles are combined with a practical engineering approach to provide a design/teaching tool that will facilitate understanding through user interaction with the simulation process.

All performance evaluation modules are built for independent modular execution in stand-alone fashion or for dependent subroutine execution called from external programs. Soon the

simulations will be turned into standard windows-type dynamic link libraries (DLLs) so they can be easily used as algorithms in other programs.

PM Motor Interactive Design Tool

DOE has granted permission for ORNL to assert copyright for the RGPM motor design tool and it is being made available to the HEV community. Below are two screen copies of the PM motor design tool, the front-end screen and the cycle-evaluation screen.

Figure F-1 is the front-end screen, which depicts the effects of varying the motor length and gear ratio, for a 30 kW motor in an electric vehicle executing the FUD cycle. Observe the change in average cycle efficiency (upper right-hand corner) when the length is increased in three steps of 1 cm each, followed by a change in gear ratio from 1:1 to 2:1, and a subsequent reduction in length, back to the original, in three steps of 1 cm each. It is clear that a gear ratio of 2:1 better uses the motor's capabilities. The cost of the gearbox versus the gain in efficiency is an important consideration. It is clear though that increasing the motor length has small impact on efficiency but significant impact on motor costs.

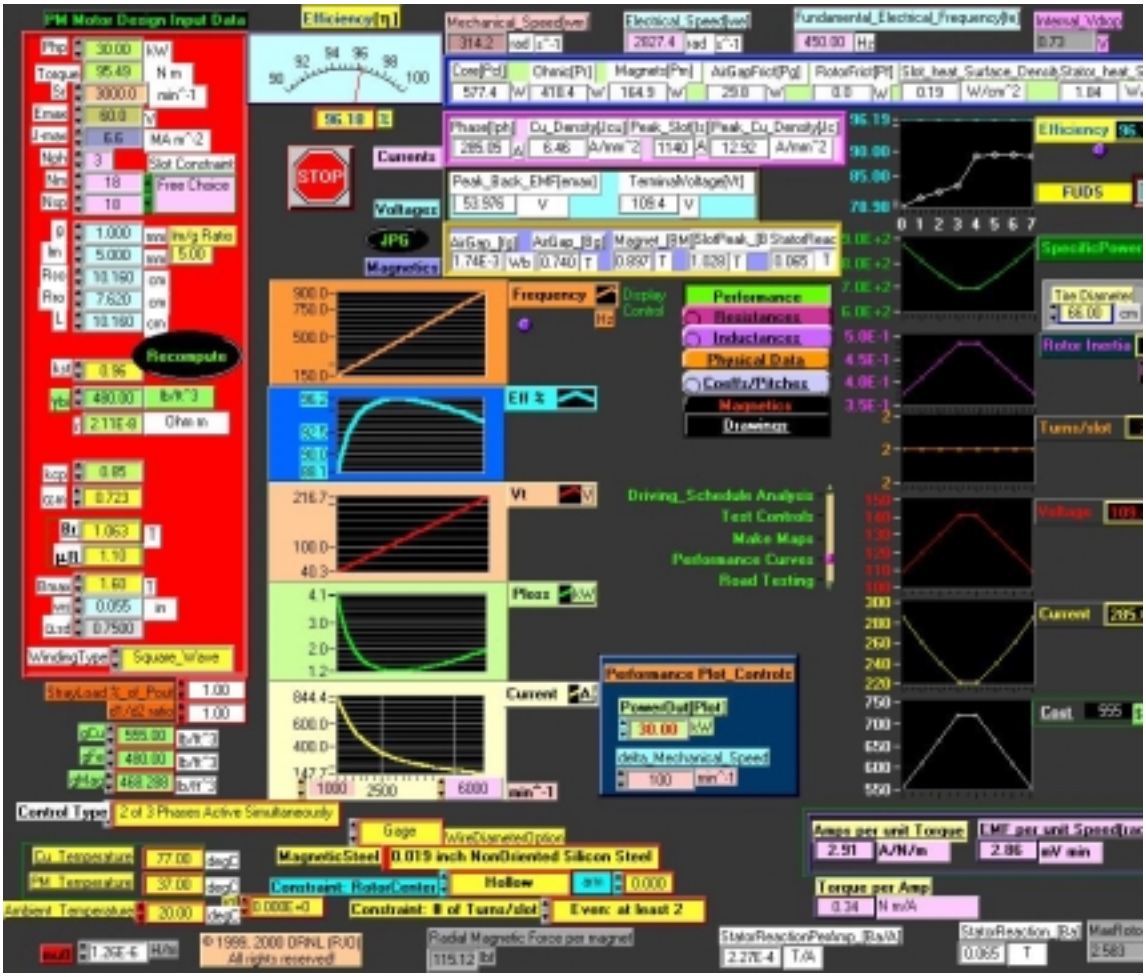

Figure F-1. Design tool's front end screen.

Figure F-2 is the screen showing the performance of the same motor configured as a parallel HEV subject to the FUD schedule. It allows assessment of the PM motor's efficiency as it navigates a driving schedule for different levels of power supplied by an ICE. Because of complex interactions between average cycle efficiency and different combinations of gear ratios, driving cycles, and level of power supplied by the ICE, the relationships are often unpredictable.

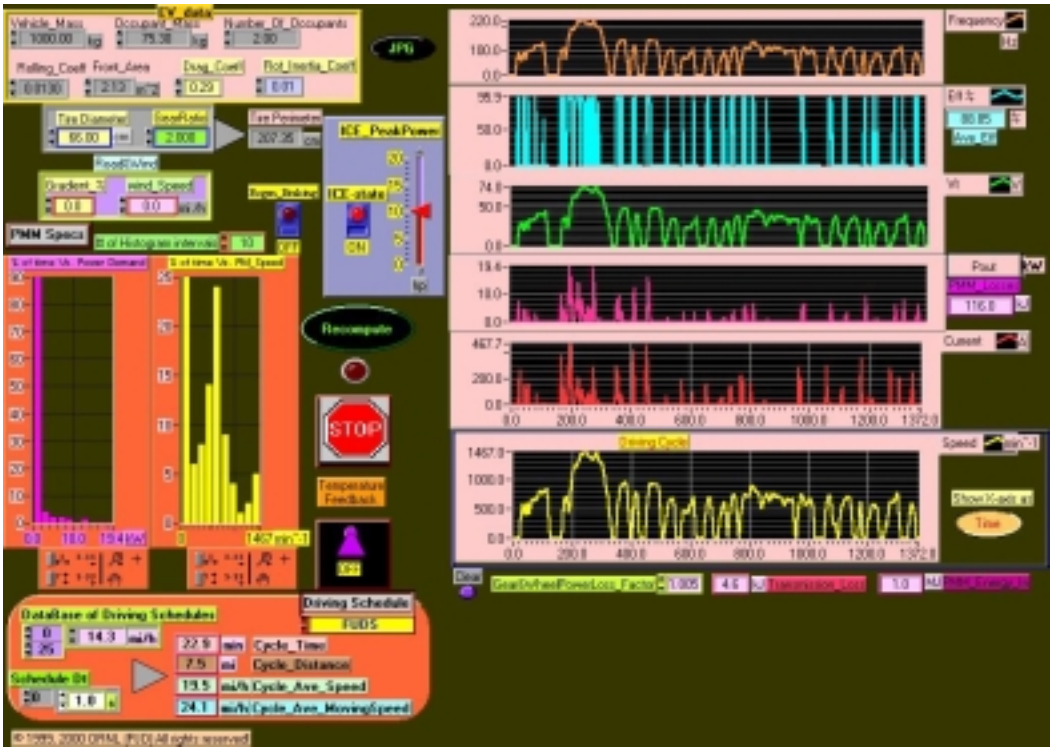

Figure F-2. Driving cycle evaluation screen.

Selection of gear ratio for highest efficiency varies dramatically with driving cycle depending on the level of power supplied by the ICE.

In Figure F-2, the internal combustion engine provides the first 10 hp of the load. Wind and road gradient are zero, regeneration is off, and the gear ratio is 2:1. A new "cycle statistics" feature in red on the left shows the percent of time the vehicle delivers a certain power and the percent of time it is at a certain speed. Note that every numeric box with up/down arrows on its side is a control element that allows the user to interactively change that value used by the simulation to provide instant feedback.

Development of SRM

Reluctance is the mathematical inverse of inductance. A reluctance motor is an electric motor in which torque is produced as its rotor moves to a position that minimizes the inductance of the stator-rotor system. When current circulates through the windings of a stator pole, the magnetic

field produced attracts a nearby rotor pole. By systematically energizing and de-energizing the stator poles, continuous rotary motion may be achieved.

The first stage in the development of our simulation follows classic algorithms to estimate the main characteristics of the motor from specified requirements and constraints. Figure F-3 shows the main screen of the first stage SRM simulator.

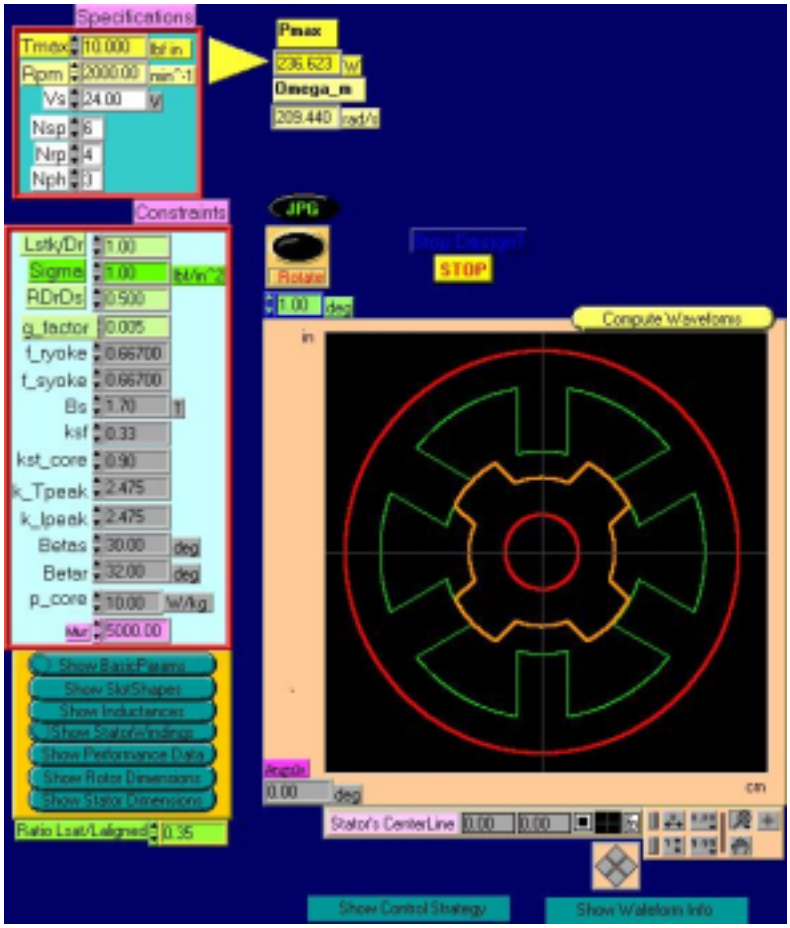

Figure F-3. Main screen of SRM.

In the second stage, the design and performance analyses are refined to solve the time-dependent fundamental equations as the rotor turns. Crucial to this refinement is the ability to compute the dependence of the system's magnetic properties from the stator current and the position of the rotor. There has been good progress in these waveform-based computations without resorting to finite-element computations.

Conclusions

ORNL's simulation work supports HEV drive system evaluation and selection by providing physics-based tools that perform several types of comparative evaluations. First, in the hands of drive system developers the tools enable comparison of fundamental design differences, of

performance at "nominal" operation over representative driving schedules, and of performance curves covering user selected speed ranges and loads. Second, the tools generate importable files to represent electric drive systems in DOE's full vehicle simulation codes. Finally, the tools guide test plan preparation and interpretation of experimental drive system characterization data.

Publications

P. J. Otaduy et al., "Model-based Generation of Scaling Laws for Radial-Gap Permanent Magnet Motors," Paper 00FCC-36 in the *Future Car Congress*, Hyatt Regency, Crystal City, Virginia, April 2–6, 2000.

References

T. J. E. Miller, *Switched Reluctance Motors and their Control*, Magna Physics Publishing and Clarendon Press, Oxford, 1993.

D. C. Hanselman, *Brushless Permanent-Magnet Motor Design*, McGraw-Hill, Inc., 1994.

P. Lawrenson et al., *Variable-Speed Switched Reluctance Motors*, *IEE Proceeding*, Vol.127, Part B, No. 4, pp. 253–265, July 1980.

A. V. Radun, "Design Consideration for the Switched Reluctance Motor," *IEEE Trans on IA*, Vol. 31, No. 5, pp.1079–1087, September/October 1995.

G. HEV Switched Reluctance Machines

John W. McKeever
Oak Ridge National Laboratory
National Transportation Research Center
2360 Cherahala Blvd.
Knoxville, Tennessee 37932
Voice: 865-946-1316; Fax 865-946-1210; mckeeverjw@ornl.gov

Objective

- To accurately assess state-of-the-art SRM and drive technology by evaluating commercially available SRM/drive systems' performance as HEV traction drive systems, especially with respect to noise generated, vibration, and torque roughness.
- To examine the larger size and cost of switched reluctance (SR) inverter when compared with the inverter of an equivalent induction motor to see if they are inherent or sufficiently reducible to support use of an SRM as an HEV traction motor.

Approach

- Secure SRMs that are potential HEV traction drive candidates for testing and prepare for evaluation.
- Compare mechanical performance of the SRM/drive system with that measured by the vendor.
- Compare sound and vibration generated by the SRM/drive systems with that generated by a baseline HEV traction drive system.
- Use a sound measuring method and a PC-based Multi-Analyzer system to quantify generated audible sound energy passing through a fixed boundary.
- Use special accelerometers to separate translation vibrations amplified by the structure from torsional vibrations that are driven by torque ripple.
- Examine the test results in light of ORNL's SRM model to identify the source of noise problems and possible solutions.

Accomplishments

- Received a 12 kW, 4-phase, 8-pole stator/6-pole rotor SRM drive system for evaluation.
- Collaborated extensively with SRM drive vendors.
- Obtained a commitment for two low-speed, high-torque, dual-rotor, double-shaft SRM drive systems.
- OEM completed preliminary measurements on the first 35 kW unit.
- Scoped a preliminary test procedure.

Future Direction

- Receive two additional SRM/drive systems for test at NTRC and locate additional vendors.
- Characterize performance as well as noise and vibration of SRM/drive systems.
- Evaluate performance, noise, and vibration of an HEV induction or PM competitor and compare with that of the SRM/drive system.
- Compare measured performance with predictions from ORNL's SRM model.
- Use ORNL's SR inverter model to explore ways to operate and package the inverter more effectively.

Introduction

The SRM drive system with its cheaper, more robust traction motor may be able to meet the cost goals of the Office of Advanced Automotive Technologies' R&D plan for the HEV. To resolve this uncertainty, ORNL has been given the responsibility to characterize HEV size SRM units. SRMs were of great international interest at the 35th IAS Annual Meeting and World Conference on Industrial Applications of Electrical Energy in early October at Rome, Italy. Twenty papers on SRM technology were presented by university researchers. There are few, if any, commercially available units that can deliver between 30 and 70 kW peak power, which is the range required by the HEV. This poses an additional challenge to locate eligible units.

In an attempt to remedy this situation, ORNL is promoting development of a viable commercial SRM drive system by providing independent evaluation of such commercial or prototype systems obtained from industry. The purpose of the evaluation is to determine if they meet the HEV standards for performance, noise, and vibration. ORNL is also prepared to collaborate with SRM vendors to guide innovations and development of SRM technology.

The simplicity of the SRM, which makes it attractive as an HEV traction motor, inherently imposes features requiring complex special equipment to gather data that will enable comparisons with other HEV drive system candidates. These features include harsh waveforms, torsional vibration caused by high torque ripple, and torque/speed curves different from those of their induction motor counterparts. If these undesirable features can be moderated or eliminated, the simplicity of the motor makes it an excellent candidate to meet cost, volume, weight, and reliability goals.

Test Instrumentation and Setup

The SRMs will be driven by inverters furnished by the OEMs. Mechanical performance will be measured by a Dyne Systems dynamometer. A bi-directional microphone shown, in Figure G-1, will measure the flow of sound energy across nodes of a boundary around the motor. This noise measuring technique does not require an anechoic chamber. Sound energy data as well as rotational, radial, and axial vibrations will be logged and analyzed with a B&K Type 3560 PC-based Multi-analyzer System, shown in Figure G-2, to obtain information that may be normalized for comparison with competing HEV drives.

Figure G-1. Directional sound measuring wand.

Figure G-2. Acoustic and vibration data acquisition. system.

SRM Drives Now Available for Testing

Figures G-3 and G-4 show the 12 kW, 4-phase, 8-stator pole/6 rotor pole drive system and its inverter. Figure G-5 is a schematic of the low-speed, high-torque, dual-rotor, double shaft, 35 kW, 3-phase, 24-stator pole/16 rotor pole drive system, designed by Magna Physics. The actual SRM is shown in Figure G-6.

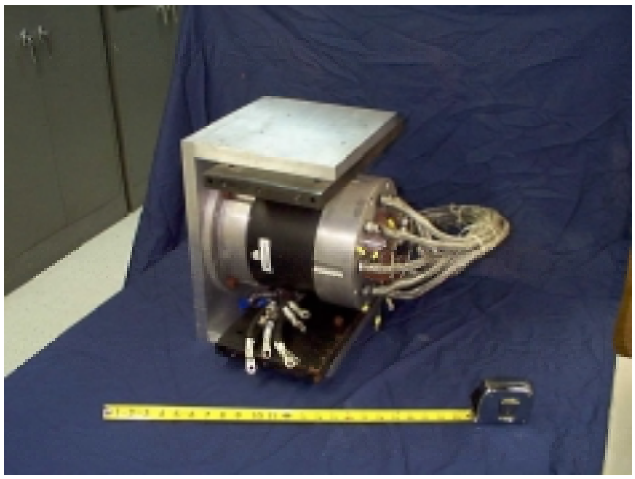

Figure G-3. 12 kW SRM.

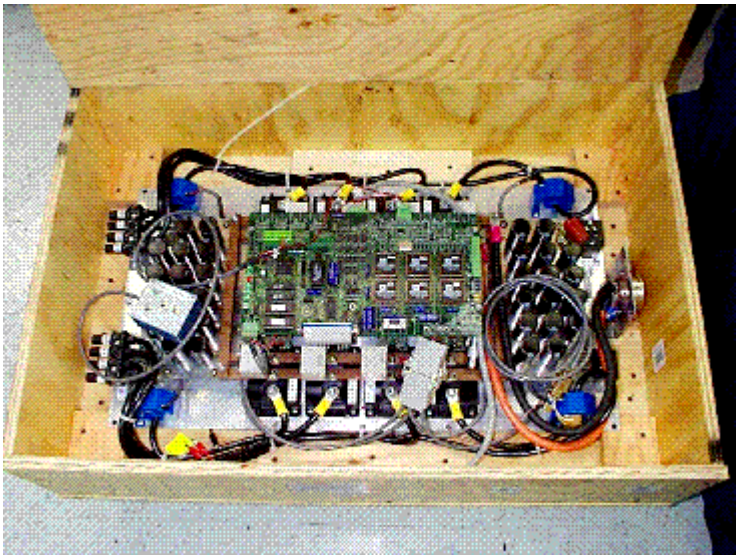

Figure C-4. Inverter drive for 12 kW SRM.

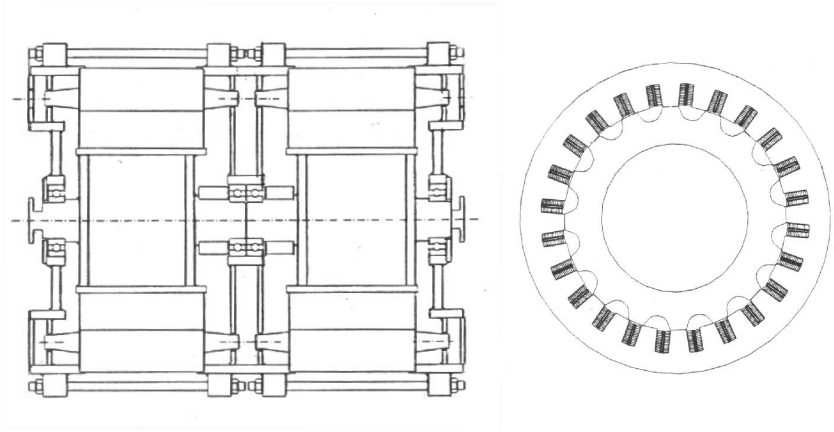

Figure G-5. Schematic of the 35 kW double shaft SRM.

Figure G-6. High-torque, dual-rotor, double shaft 35 kW SRM.

Preliminary SRM Evaluation

The OEM that provided the 35 kW SRM completed some preliminary mechanical characterization in July 2000. The motor and mounts weigh 247 kg and occupy 0.044 m^3 (45.4 L) and the dc phase resistance is 73.3 mΩ. Table 1 summarizes some performance data at the 500 rpm base speed. The motoring performance parameters exceed the design specifications; however, the motor's specific power at peak load is 0.15 kW/kg, which is about 9% of the 1.6 kW/kg PNGV goal, and the volumetric power density is 0.84 kW/L, which is about 17% of the 5 kW/L PNGV goal. ORNL modeling of the SRM may be able to suggest ways to align this design more favorably with PNGV goals. Note that the regeneration efficiencies for continuous and peak torques are significantly lower than the motoring efficiencies, a measurement, which if confirmed, will have to be investigated.

Table G-1. Performance parameters of high-torque, dual-rotor, double shaft, 35 kW SRM

Feature	Design Specs.	Motoring Measurement	Regeneration Measurement
Continuous rated torque, N-m	334	362	380
Continuous rated power, kW	17.5	20	20
Peak torque, N-m	668	720	640
Peak power, kW	35	38	35
Efficiency, % @ cont. rated torque	blank	87	74
Efficiency, % @ peak torque	blank	74	59

Additional measurements by the OEM provided the following information.

- Flux linkages were calculated as a function of current from time plots of voltage and current. Flux linkage data was then used to calculate static torque of the machine. Maximum torque of 780 N-m occurred at 125 electrical degrees.
- The dynamometer rotated the motor to determine its spin losses with the inverter off. At 1400 rpm the power loss was less than 166 W.
- Thermal tests identified the hot spots and maximum temperature rises
  - A static (stationary rotor producing no torque) test passed sufficient current through stators of both motors to simulate rated power dissipation during operation. Maximum temperature rise was 24.3 C° over a 29-minute period during which ethylene glycol water coolant at 65 °C was delivered at 5 gal/min.
  - Half the motor was used in a dynamic test to deliver 31.5 kW during which the maximum temperature rise was about 33 °C under the same cooling conditions.
  - During a 90 s peak load delivery the hot spot temperature rose 71°C to 126°C.
- With the rotor locked, accelerometers mounted on the stator outer surface showed one dominant stator vibration mode when one stator phase was pulsed to its peak current. The modal frequency is about 700 Hz.
- Below 100 rpm the acoustic noise is very low. Above 100 rpm noise increases mainly due to torque ripple. Waveform measurements show that the third harmonic of the excitation lies near the stator mechanical frequency.

Anticipated Testing by ORNL

ORNL will use facilities similar to those used for AEMD evaluation for performance confirmation and testing with special emphasis on quantifying vibration, and noise for comparison. Similar tests on competing HEV motor systems will be made to provide data for comparison.

- Preliminary – Bench measurements of stator winding dc resistance and inductance as a function of angle will probably be used to assure motor integrity after transit.
- Performance – A dynamometer will be used to confirm vendor performance data. Inverter dc link voltage and dc current, inverter output voltage and current, SRM speed, torque, and mechanical power delivered to the dynamometer will all be measured for several motoring cases. These cases include the torque speed envelope for maximum, nominal, and minimum voltages at maximum load, 50% load, and no load. Corresponding measurements will be taken for regeneration cases. Spin-down losses will be measured and the waveform of cogging torque versus angle will be captured at the lowest measurable speed.
- Thermal responses – Temperature responses of the motor and controller will be measured at continuous rated power and at peak power. A static test may be adequate for continuous rated power. Peak power for 90 s will probably require a dynamic test.
- Noise – Flow of sound energy through a surface bounding the motor will be measured with special sound measuring equipment. Background noise with the motor at rest will be measured first. This will be subtracted from the noise measured when the motor is running under load. Several bounding envelopes will be measured to check internal consistency.

- Vibration – Special instrumented motor mounts will be used to separate radial frame vibrations from torsional shaft vibrations.

Inverter for the SRM

On the basis of existing literature, the inverter for the SRM is larger and the cost is greater than that of an inverter for an equivalent induction motor. At least part of the cost is related to the nature of the SRM that operates using short precisely controlled duty cycles and higher current. Examination of the SRM inverter's operation using ORNL's SRM/inverter model may provide insight leading to more effective ways to operate the inverter and ways to reduce its cost. The question is whether today's size and cost penalties are inherent in the nature of the SRM drive system or may be overcome by engineering optimization in time to be used as an HEV traction drive system.

Conclusions

The SRM drive system may be able to meet OAAT R&D cost goals and PNGV performance, noise, and vibration limitations. Since the inverter drive is inherently large and expensive, research to reduce these unfriendly parameters will be pursued. This project is geared to increase the probability that an eligible HEV traction system will be available for selection and accompanied by test data to evidence that eligibility. Probability of success is further increased by three technologies being advanced at ORNL. The first is SRM modeling technology and design experience, which provide a foundation for collaboration with the SRM drive system OEMs to make suggestions for improved SRM systems that meet PNGV goals. The second is ORNL's motor test experience, which provides a basis for evaluating test results and assisting the PNGV to select the most promising HEV drive system candidates. The third is ORNL's experience with drive inverters for induction and PM motors, which may now be applied to the SRM.

H. Automotive Electric Motor Drive (AEMD) Validation Testing and Contract Support

Curtis W. Ayers
Oak Ridge National Laboratory
National Transportation Research Center
2360 Cherahala Boulevard
Knoxville, Tennessee 37932
Voice: 865-946-1342; Fax: 865-946-1210; ayerscw@ornl.gov

Objectives

- Provide technical support to the AEMD Contracts Manager
- Planning and organization of the testing phases of the AEMD program
- Produce a plan for testing, identify and purchase the equipment and instruments required to meet the needs of the test plan
- Develop software for controlling the AEMD load profiles for various tests
- Procure and assemble the test stand and perform preliminary tests

Approach

The conformance to established standards will be assessed and the results will be utilized to determine the suitability of the AIPM technology for automotive applications.

Accomplishments

- Referenced test standards and pertinent documents have been acquired.
- Environmental test procedures have been completed.
- The development of the functional test and electrical characterization tests are ongoing.

Future Direction

The AEMD must be designed and manufactured to overcome cost, volume, weight, and thermal and reliability barriers in order to meet technical targets. This project will verify the suppliers/developers success in accomplishing these ends.

Introduction

The AEMD sub-task supports DOE's program effort to research, develop, and demonstrate a traction motor for use in advanced hybrid electric vehicles that meets the goals and schedule of PNGV. The overall objective is to sponsor a commercially viable electric motor technology that contributes to the goal of having a passenger vehicle with three times the fuel economy of present vehicles. Requirements for the traction motor to achieve this goal will require reduction of the size and weight, reduction of the manufacturing cost, and improvements in the efficiency and reliability.

ORNL's role for the AEMD project are to provide technical support to DOE, plan and organize the testing phases of the AEMD program, and validate conformance with the AEMD specification requirements. ORNL will produce a plan for testing of the AEMD pre-production prototypes according to the specifications and standard test procedures called out in the solicitation. ORNL will specify the equipment and instrumentation required to meet the needs of the test plan when the required test method details have been established. The most cost effective methods of testing the AEMDs will be considered in the decision to purchase test equipment, leverage use of equipment from related work, or utilize facilities elsewhere. A large portion of the testing facilities and procedures will be leveraged from the AIPM project. This sub-task will include software development for controlling the AEMD load profiles for various tests. ORNL will perform the required configuring, assembling, etc., for testing fixtures to support the developed test method(s). The sub-task will include some preliminary testing of the systems in preparation of the actual AEMD testing and any necessary refinement of the test procedures. It is anticipated that the AEMD contract motors will become available at ORNL in the first quarter of FY 2002.

ORNL activities for FY 2000 were to develop the required testing methods, specify and procure instrumentation and equipment to perform the testing, and provide technical support to the contract manager. In addition, questions concerning the AEMD specification and solicitation involving current and power levels as well as specific environmental tests are being resolved. Recommended changes to the AEMD specifications have been submitted to the program participants for review and some comments have been received.

ORNL activities for FY 2001 will be to refine test methods to specific AEMD test articles, specify and procure additional instrumentation and equipment, assemble the equipment and/or instrumentation in the configurations needed for the various tests, and provide support to the Contracts Manager.

I. Real-Time Platform for the Evaluation of Electric Machinery Control Algorithms

John Chiasson
The University of Tennessee
Knoxville, Tennessee 37996-2100
Voice: 865-974-0627; Fax: 865-974-5483; chiasson@utk.edu

Leon Tolbert
Oak Ridge National Laboratory
National Transportation Research Center
2360 Cherahala Boulevard
Knoxville, Tennessee 37932
Voice: 865-946-1332; Fax: 865-946-1262; tolbertlm@ornl.gov

Objective

- Develop and test advanced control and modeling algorithms for the various types of motor drives considered for HEVs.

Approach

- Prepare a library of SIMULINK control/modeling algorithm blocks that can easily be implemented in a real-time test environment for induction motors, SRMs, and PMSMs.
- Bypass the need for specialized programming in C or assembly languages so that investigators can spend their time intensively studying proposed control algorithms.

Accomplishments

- Developed a "skeleton" library of SIMULINK files to allow users to have at hand state-of-the-art algorithms for the feedback control of the PM synchronous and variable reluctance motors.
- Purchased computer hardware and software, motors, inverter, and other equipment with University of Tennessee equipment grant. Set up computer control and data acquisition hardware.
- Assembled inverter components (current sensors, heat sink, power supply, gate drivers, and main device module) and motor test stand (test motors, torque sensor, and load motor).
- Developed new algorithms for obtaining the maximum torque as a function of speed in PMSMs subject to voltage and current constraints. This work has been submitted for publication and presentation at the 2001 American Control Conference.

Future Direction

- Develop a "skeleton" library of SIMULINK files for state-of-the-art algorithms for the feedback control of induction motors.
- Develop a set of sophisticated computer algorithms (SIMULINK files) that include sensorless techniques for automatic machine parameter identification, automatic tuning of the controller parameters, and fault diagnosis algorithms.
- Test algorithms with the three different machines being considered for HEVs: Induction Motor, PMSM, and SRM.

Introduction

The dc motor, induction motor, PMSM, and the SRM have all been proposed for HEV propulsion. The issue of which motor to use for the propulsion of electric vehicles is still unresolved because the cost, performance, reliability, size, and efficiency all play a large role in the decision and no one motor can presently be said to be the "best" choice. Each of these motors are quite different in the their operation and each requires a specialized computer controller (software program) to determine when the electronic switches of the power inverter should switch to produce the appropriate voltages applied to the motor to achieve the requested torque.

The primary function of a motor is to provide torque and, consequently, control schemes are developed to provide torque control based on feedback of the motor currents and rotor position/speed. However, the control of the electric motor for an HEV not only includes the basic feedback controller to achieve torque control, but also more advanced capabilities including automatic identification of motor parameters, self-tuning of the controller gains, fault diagnosis to determine failures, etc. Further, an encoder is presently required for high-performance control of all motors but the dc brush motor. The encoder is an additional cost and often has reliability problems. Though the dc motor requires only a simple controller without the use of an encoder, it is not regarded as a viable choice because the required maintenance of its commutator and brushes outweighs these advantages. Consequently, there is a lot of interest in sensorless control of the above three ac motors.

The work reported here is the development of a real-time computing platform that provides a convenient way to evaluate the variety of software controllers that are under consideration for HEVs. This approach bypasses the need for specialized programming in C or Assembly Languages and instead allows investigators to spend their time intensively studying the proposed control algorithms.

Accomplishments

The Phase I part of the project was only three months in duration. Although faced with delays by vendors in the delivery of their equipment as well as the short time span of the first phase, much progress was made in the project.

The Real-Time Platform

Most of the basic equipment for the real-time platform has been procured and set up[1]. Shown in Figure I-1 is a block diagram of the real-time evaluation platform that has been setup. As seen in the figure, the software side of the evaluation platform consists of a host computer (PC) and two target computers (PCs). The host computer is used to design the motor/converter controller in a block diagram form using MATLAB/SIMULINK software provided by Mathworks, Inc. The SIMULINK block diagram controller design for the motor or power electronic controller is then converted to C code using the REAL-TIME WORKSHOP (RTW) software. Finally, using specialized software developed by OPAL-RT Inc., this C code is converted to executable code to run on the two target computers under the QNX operating system. The OPAL-RT system provides real-time communication and synchronization between the two target computers and also allows data to be sent back and forth in real-time between the host computer and the two target computers with the data displayed using LABVIEW software on the host computer. An interface board in each target computer reads in the information (voltages, currents, speed, position, temperature, etc.) from the motor needed by the control program and sends out the commands to the power electronics as determined by the controller. The platform is now undergoing testing to validate that the A/Ds, D/As, encoder, target, and host computers are all communicating properly. A coupling mechanism between the load and various test motors is close to completion.

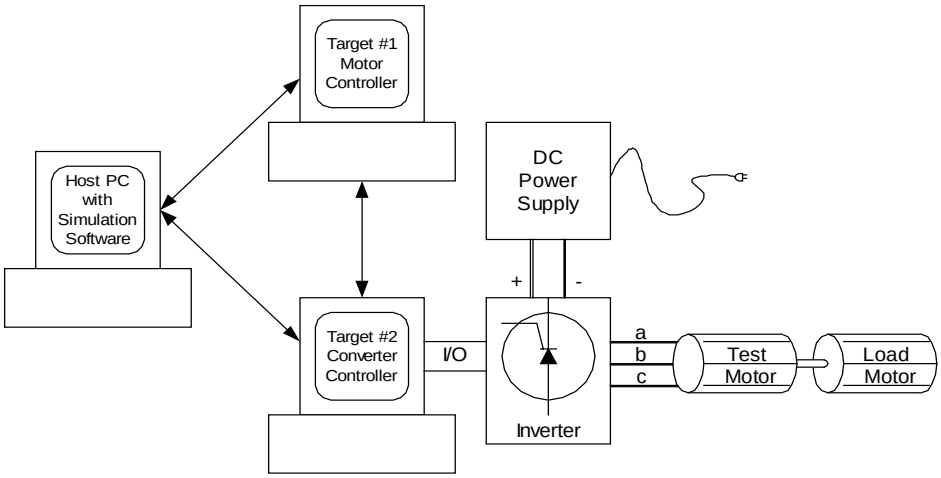

Figure I-1. Software side of the evaluation platform consists of a host computer (PC) and two target computers (PCs).

[1] We are currently waiting for the vendor software that allows real-time communication between the two target computers. The vendor Opal-RT has developed real-time software to run on standard PCs and communication between target computers in real-time via FIREWIRE. The new software being developed by OPAL-RT will allow real-time communication between the two target computers via GIGANET boards providing much higher performance.

The SIMULINK Models

SIMULINK models of the controllers for the switched reluctance and PM synchronous motors have been completed.

SRM

Specifically, the SIMULINK blocks that have been developed are: (a) a state-of-the-art controller that does balanced current commutation[2],[3]; (b) a model identification scheme that allows one to automatically (experimentally) identify the torque vs. current/position curves of the SRM; (c) a full simulation model of the SRM for off line simulation; and (d) a smooth trajectory generator for a speed/position profile with the final speed/position chosen by the user.

A block diagram of the SRM control simulation is shown in Figure I-2. To use this simulation for real-time control, one simply removes the "SRM" block and replaces it with an output block (provided by Opal-RT) that provides the software to send the voltage commands to the amplifiers and an input block (provided by Opal-RT) that provides the software to bring in the measured currents and encoder data. An initialization file provides all the parameters for the motor, inverter and trajectory for the particular application. Using the Opal-RT software, one simply clicks on buttons to compile this SIMULINK model to C code and then on to machine code, load it to the target computers and then execute it in real-time.

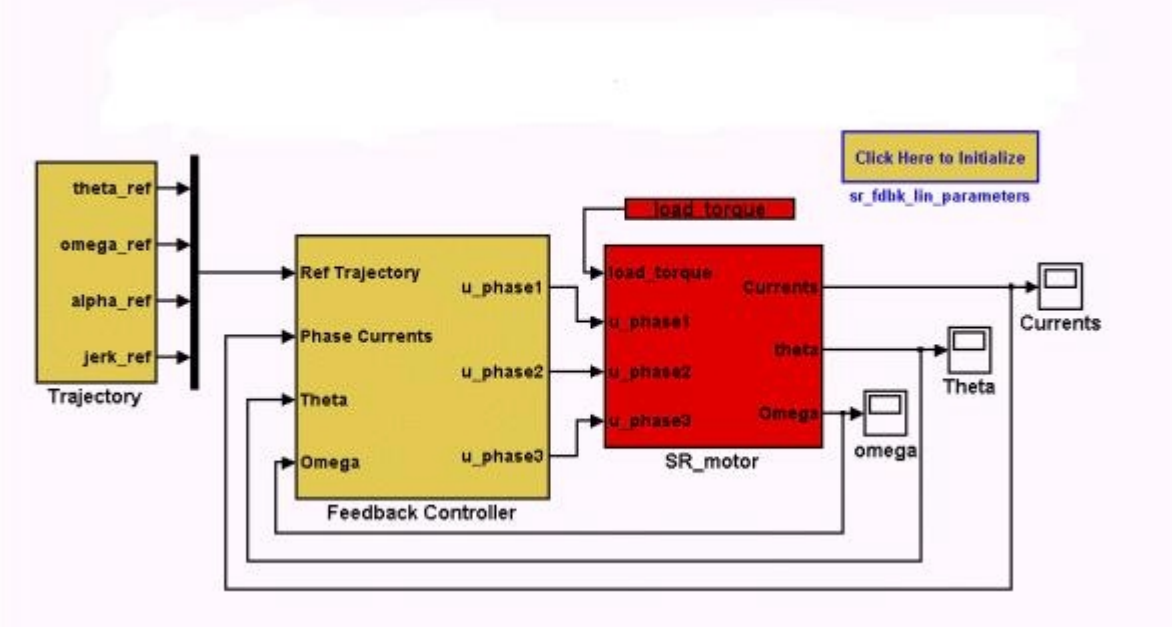

Figure I-2. Simulation of a SRM with a feedback linearization controller.

The controller, indicated by the block diagram in Figure I-2, is quite complex. By "double clicking" on the "feedback controller" block, one finds the block diagram shown in Figure I-3. One may keep clicking into each block to its most primitive level.

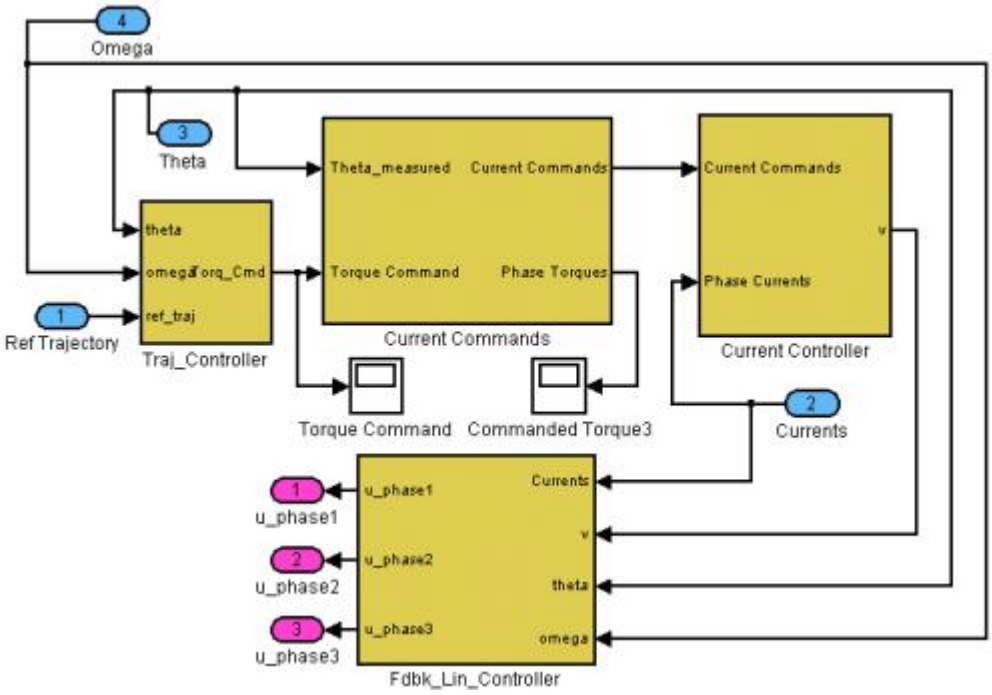

Figure I-3. Expansion of feedback controller block.

This particular controller is referred to as "feedback linearization[3]." However, a high-gain current command controller has also been developed[9], and one simply replaces the above "feedback controller" block with the "high-gain" block to use it.

PMSM

Similarly, SIMULINK models of the controllers for a PMSM have been developed. Specifically, the SIMULINK blocks that have been created are: (a) a state-of-the-art field-oriented feedback controller[4,5]; (b) an identification scheme to estimate the model parameters[6]; and (c) a smooth trajectory generator for a speed/position profile with the final speed/position chosen by the user.

A block diagram at the highest level of the PMSM control simulation is shown in Figure I-4. Again, to use this simulation for real-time control, one simply removes the "three-phase model PMSM" block and replaces it with an output block (provided by Opal-RT) that provides the software to send the voltage commands to the amplifiers and an input block (provided by Opal-RT) that provides the software to bring in the measured currents and encoder data. Moreover, the Opal-RT software allows this to be transparent to the user.

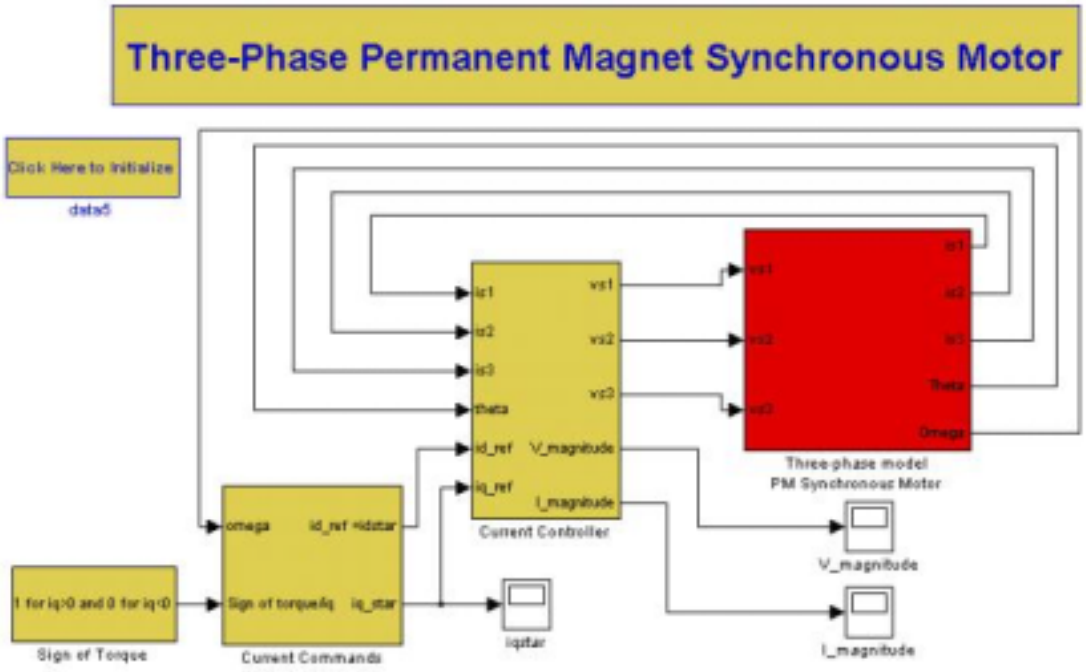

Figure I-4. Three-phase PMSM control block diagram.

Double clicking on the "current controller" results in the block shown in Figure I-5.

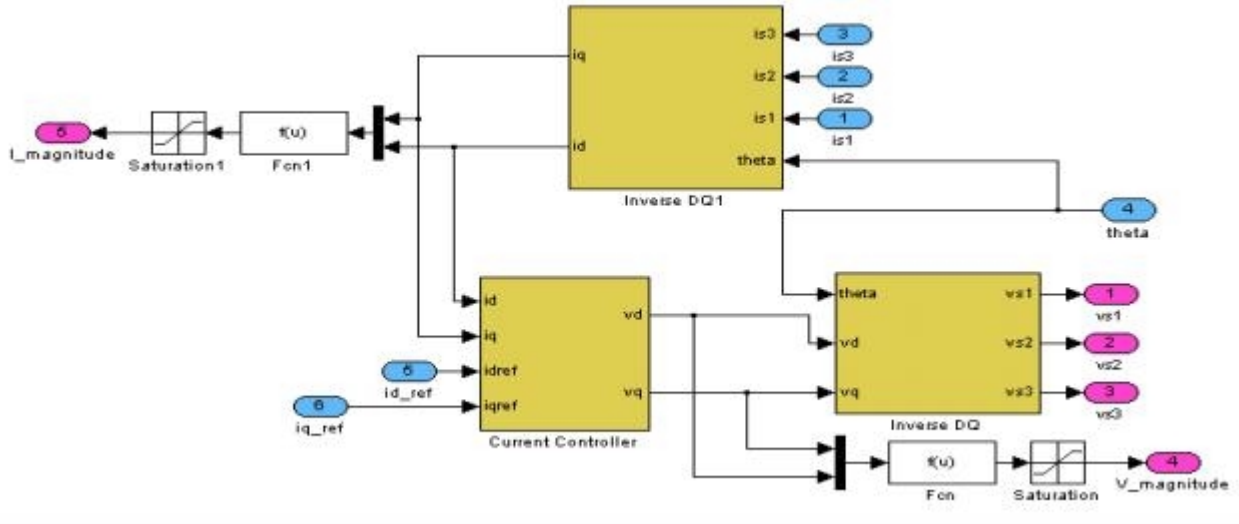

Figure I-5. Expansion of the current controller block in Figure I-4.

The above controller is a standard dq controller for torque control[4,5] with additional special look-up tables provided to give the direct and quadrature currents as a function of speed that produce the maximum torque possible without violating the voltage and current constraints[1]. We have also produced a controller for position and speed control as in Ref. 4 and identification of the motor parameters are carried out as in Ref. 6.

Future Direction

A skeleton set of SIMULINK models are to be developed for the induction motor including (a) a state of the art field-oriented feedback controller; (b) a rotor flux estimator; and (c) an identification scheme to estimate the model parameters.

The above sets of SIMULINK models for the SRM, PM, and Induction Motors are to be fully tested on the real-time computing platform.

After fully testing the above, it is proposed to develop and test new SIMULINK blocks for various functions for HEV propulsion systems. These include:

SRM

An optimized current commutation controller for minimum energy loss.
An optimized current commutation controller for minimum di/dt.
A set of blocks for various sensorless control schemes.

Induction Motor

A set of blocks for various sensorless schemes for field-oriented feedback control.
An adaptive scheme for rotor time constant and load torque variations.

PMSM

A set of blocks for various sensorless schemes for field-oriented feedback controller.
An identification scheme to estimate the model parameters.

Power Electronics

Carrier-based PWM.
Space vector PWM.
Harmonic elimination based PWM.

Note that these blocks in Phase II have much more of a research/development flavor in that, e.g., no accepted (standardized) methods exist for sensorless control. Consequently, several different blocks corresponding to different approaches will be developed.

References

1. M. Bodson, J. Chiasson, and L. Tolbert, "A Complete Characterization of Torque Maximization for Permanent Magnet Non-Salient Synchronous Motors," submitted to the 2001 American Control Conference.
2. R. S. Wallace and D. G. Taylor, "A Balanced Commutator for Switched Reluctance Motors to Reduce Torque Ripple," *Transactions on Power Electronics*, Vol. 7, No. 4, October 1992.
3. M. Ilic-Spong, R. Marion, S. Peresada, and D. G. Taylor, "Feedback Linearizing Control of Switched Reluctance Motors," *IEEE Transactions on Automatic Control*, Vol. 32, No. 5, May 1987.

4. M. Bodson, J. N. Chiasson, R. T. Novotnak, and R.B. Rekowski, "High-Performance Nonlinear Feedback Control of a Permanent Magnet Stepper Motor," pp. 5–14 in *IEEE Trans. on Control Systems Technology*, Vol. 1, No. 1., 1993.
5. W. Leonhard, *Control of Electrical Drives*, Springer Verlag, Berlin, 1990.
6. A. Blauch, M. Bodson, and J. Chiasson, "High-Speed Parameter Estimation of Stepper Motors," pp. 270–279 in *IEEE Trans. on Control Systems Technology*, Vol. 1, No. 4, 1993.
7. M. Bodson, J. Chiasson, and R. T. Novotnak, "A Systematic Approach to Selecting Optimal Flux References in Induction Motors," pp. 388–397 in *IEEE Trans. Control Systems Technology*, Vol. 3, No. 4, 1995.
8. J. S. Lawler, J. M. Bailey, and J. W. McKeever, *Extended Constant Power Speed Range of the Brushless DC Motor Through Dual Mode Inverter Control*, Oak Ridge National Laboratory, ORNL/TM-2000/130, 2000.
9. D. G. Taylor, "An Experimental Study on Composite Control of Switched Reluctance Motors," *IEEE Control Systems*, February 1991.